

10-3-1995

Electrostatic Interactions at Membrane-water Interfaces and Distribution of 2, 4, 6-Trichlorophenol in a Membrane Model System

Isolde Sieder
Portland State University

Follow this and additional works at: https://pdxscholar.library.pdx.edu/open_access_etds



Part of the [Physics Commons](#)

Let us know how access to this document benefits you.

Recommended Citation

Sieder, Isolde, "Electrostatic Interactions at Membrane-water Interfaces and Distribution of 2, 4, 6-Trichlorophenol in a Membrane Model System" (1995). *Dissertations and Theses*. Paper 5087. <https://doi.org/10.15760/etd.6963>

This Thesis is brought to you for free and open access. It has been accepted for inclusion in Dissertations and Theses by an authorized administrator of PDXScholar. Please contact us if we can make this document more accessible: pdxscholar@pdx.edu.

THESIS APPROVAL

The abstract and thesis of Isolde Sieder for the Master of Science in Physics were presented October 3, 1995, and accepted by the thesis committee and the department.

COMMITTEE APPROVALS:



Pavel Smejtek, Chair

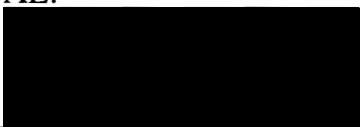


Jonathan Abramson



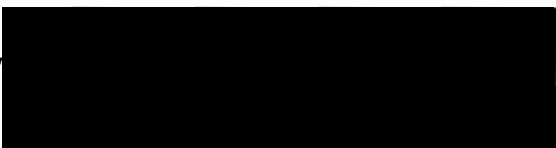
Robert Millette
Representative of the Office of Graduate Studies

DEPARTMENT APPROVAL:



Erik Bodegom, Chair
Department of Physics

ACCEPTED FOR PORTLAND STATE UNIVERSITY BY THE LIBRARY

by  on 28 November 1995

Abstract

An abstract of the thesis of Isolde Sieder for the Master of Science in Physics presented October 3, 1995.

Title: Electrostatic Interactions at Membrane-Water Interfaces and Distribution of 2,4,6-Trichlorophenol in a Membrane Model System

It is generally accepted that biological membranes consist of a lipid bilayer matrix with proteins incorporated into the lipid bilayer. Typically, these membranes are negatively charged due to the presence of negatively charged lipids in the bilayer as well as negatively charged molecular groups on proteins. Biologically active molecules, such as environmental pollutants, enter the membrane from the aqueous phase by adsorption or partitioning into the lipid bilayer. The thesis consists of two parts.

Part I is a computational study of spatial distribution of electric potential in the aqueous portion of the membrane-water interface using two models of charge distribution: (i) the discrete charge model, in which charges are located on a square lattice either on the surface or embedded in the membrane: (ii) the

continuous charge density (smeared charge), Gouy-Chapman, model in which the charge is assumed to be evenly spread on the membrane surface. The computed distributions of electric potential are used to predict spatial distributions of positively charged hexavalent cation of Ruthenium Red (RuR) at the membrane-water interface. It was found that anomalous behavior of RuR cannot be explained by this version of the discrete charge theory.

Part II is concerned with the distribution of ionized and un-ionized species of 2,4,6-Trichlorophenol (2,4,6-TrCP) in octanol-water system, which is often used as an experimental model for predicting the distribution of toxic chemicals in the environment. In this experimental study we obtained the pH dependence of the total distribution coefficient of 2,4,6-TrCP from which the octanol water partition coefficients of the un-ionized and ionized species were determined. We compared the octanol-water partition coefficient of several chlorophenols with experimental data on adsorption of ionized chlorophenols to lipid membranes. It was found that the membrane-water partition coefficient of ionized 2,4,6-TrCP is about 240 greater than that predicted from the octanol-water system. This finding supports the hypothesis that octanol-water partition coefficients cannot be used for predicting concentrations of ionized species of chlorophenols in lipid membranes.

ELECTROSTATIC INTERACTIONS AT
MEMBRANE-WATER INTERFACES
AND
DISTRIBUTION OF 2,4,6-TRICHLOROPHENOL
IN A MEMBRANE MODEL SYSTEM

by

ISOLDE SIEDER

A thesis submitted in partial fulfillment of the
requirements for the degree of

MASTER OF SCIENCE
in
PHYSICS

Portland State University
1995

Für
meine Eltern Gretel und Gerhard
und mein Bruder Georg

Acknowledgments

First and most of all I would like to thank my advisor Prof. Pavel Smejtek. It was a great pleasure to work with him. His excitement about physics, his steady flux in producing physical ideas, and his finding of new papers of interest motivated me to search more and deeper into physics. With his scientific knowledge and humorous personality he helped me to accomplish this work and always created a relaxed working atmosphere.

The experiments would not have been possible without the encouraging help of Prof. Shanru Wang. She taught me all the necessary chemical techniques and was always willing to help me with experimental problems. The availability of the centrifuges in Prof. Bob Millette's lab contributed significantly to finish the experiments on time, thanks to the lab members and their tolerance of the smell of octanol.

I enjoyed working with Piet Schmidt and Rob Ward in our lab. Serious discussions as jokes about our experiments and frustration as well as laughter was always present in our lab. Special thanks to Piet who helped me to overcome my struggles with computers and computer programs.

I also want to thank Prof. Jonathan Abramson who helped me through his biophysics lecture to get started in this field of physics which was totally new for me. I would especially like to thank Prof. Eric Bodegom who found ways to support me financially. I appreciated the help of Margie Fyfield, she helped me overcome my struggles with the English language but, furthermore, motivated me enormous to finish my thesis. She and all my friends, here and in Germany, cheered me up and helped me in my busiest time in so many different

ways. Thank you all !

Finally I want to thank my parents and my brother very much for their financial and mentally support through this year. I never will forget my great experiences here in the USA !

Contents

Acknowledgments	vi
Introduction	1
I Electrostatic Interactions at Membrane-Water Interfaces	4
1 Theory	5
1.1 The Gouy-Chapman Theory	5
1.2 The Discrete Charge Theory	9
1.3. The Boltzmann Factor	15
2 Electrical Potential and Ion Concentration Distribution in the Vicinity of the Charged Membrane Surface	16
2.1 Computations	16
2.2 Results.....	18

II	Distribution of 2,4,6-Trichlorophenol in a Membrane Model System	29
3	Introduction	30
4	Theory	37
4.1	Partition of Un-ionized and Ionized Molecules between Water and a Medium of Low Polarity	37
4.1.1	Ideal Partitioning.....	38
4.1.2	The Octanol-Water System.....	42
	a) Description of the Bulk Phases.....	42
	b) Distribution of Ionized and Un-ionized Species Between the Two Phases	44
4.1.3	The Water-Membrane System	46
4.2	Spectrophotometric Measurements.....	48
4.2.1	Lambert-Beer's-Law.....	49
4.2.2	Solvent Effects	51
5	Materials and Methods	52
5.1	Chemicals.....	52
5.2	Instruments and their Specifications	52
5.3	Preparation of Octanol and Aqueous Phases	53
5.4	Extinction Coefficients	56
5.5	Partitioning.....	57

6	Results	59
6.1	Extinction Coefficients	59
6.1.1	Results.....	59
6.1.2	Error Calculations	60
6.2	Partitioning.....	63
6.2.1	Results.....	63
6.2.2	Error Calculations	66
7	Discussion	72
7.1	Comparison of the Octanol-Water System with the Membrane-Water System	72
	Appendix A	
	Derivations: the Gouy-Chapman Theory	75
	Appendix B	
	The Partitioning in the Octanol-Water System: Multicomponent Partitioning	78
	References	82

List of Tables

1	Extinction coefficients of 2,4,6-TrCP in buffer	62
2	Extinction coefficients of 2,4,6-TrCP in water-saturated octanol	62
3	Experimental data for the pH dependence of the total distribution coefficient of 2,4,6-TrCP	67
4	Experimental data of the total concentrations of 2,4,6-TrCP in buffer and octanol (initial concentration = 20 mM)	69
5	Experimental data of the total concentrations of 2,4,6-TrCP in buffer and octanol (initial concentration = 64 mM)	69
6	Comparison of bulk partition coefficients of three different chlorophenols for lipid-membrane-water and octanol-water systems	73

List of Figures

1	Conceptual model and molecular structure of phosphatidylcholine	3
2	Fluid mosaic model of a biological membrane	3
3	Membrane model used in the Gouy-Chapman theory	5
4	Membrane model used in the discrete charge theory	10
5	Potential profiles for the discrete charge model	22
6	Concentration profiles for the discrete charge model	23
7	Potentials as a function of distance from the membrane for the studied models	24
8	Discrete charge potential as a function of embedding depth	25
9	Potentials as a function of surface charge density	26
10	Boltzmann factors as a function of distance from the membrane	27
11	Boltzmann factors for various embedding depth and charge density	28
12	Molecular structure of 2,4,6-Trichlorophenol	30
13	Energy level diagram of a diatomic molecule	49
14	Typical spectrum of the saturated buffer phase	55
15	Typical spectrum of the saturated octanol phase	55
16	Spectrum of un-ionized 2,4,6-TrCP in water-saturated octanol	61

17	Spectrum of ionized 2,4,6-TrCP in octanol-saturated buffer.....	61
18	pH dependence of the total distribution coefficient D of 2,4,6-TrCP.....	68
19	pH dependence of 2,4,6-TrCP concentrations in buffer and octanol (initial concentration = 20 mM).....	70
20	pH dependence of 2,4,6-TrCP concentrations in buffer and octanol (initial concentration = 64 mM).....	71

Introduction

Biological membranes are essential for all forms of life; in addition to separating cells from their environment they give cells their individuality needed to perform specific functions. Biological membranes are highly selective permeability barriers rather than impervious walls (Stryer, 1981). They play an important role in biological communication since they are able to process or generate chemical or electrical signals. Photosynthesis and oxidative phosphorylation, the most important biological energy conversion processes, are also carried out by membranes.

Biological membranes are sheetlike structures which consist mainly of lipids and proteins. The lipids are amphipathic molecules. They contain a hydrophilic headgroup and a hydrophobic $-(CH_2)-$ chain and can be neutral or charged. The molecular structure of a typical lipid, phosphatidylcholine, is shown in Figure 1. The lipids in the membrane are arranged as a bilayer and provide a suitable environment for proteins embedded in the membrane bilayer. Figure 2 shows the fluid mosaic model of a biological membrane, a model proposed by Singer and Nicolson (1972), generally accepted to describe the gross organization of biological membranes. Membrane proteins perform specific functions, they serve as pumps, gates, receptors, energy transducers, and enzymes (Stryer, 1981). Attempts are being made to understand complex functions of membranes in terms of laws of physics and chemistry.

Lipid bilayer is a structural element common to all biological membranes. This thesis is focused on two aspects of physical properties of lipid bilayers and on the interaction of toxic environmental pollutants with membranes:

- (1) The distribution of electric potential on the aqueous side of membrane water interface in the presence of discrete electric charges at or below the membrane surface. The importance of understanding the electric potential distribution in this region is that it determines the local concentrations of charged molecules at the membrane surface.

- (2) The distribution of un-ionized and ionized species of 2,4,6-Trichlorophenol between water and octanol. The octanol-water system is frequently used as a simple model to predict the distribution of toxic compounds in environmentally relevant systems. Serious concerns have been raised recently about its applicability, as an experimental model, to predict distributions of ionized toxic compounds between water and lipid membranes.

Part I

Electrostatic Interactions at Membrane- Water Interfaces

1 Theory

1.1 The Gouy-Chapman Theory

Gouy (1910) and Chapman (1913) proposed independently the so-called diffuse double layer theory of plane interfaces. Their theory provides an understanding of a variety of electrostatic problems associated with plane interfaces. In the case of the water-membrane interface, the *Gouy-Chapman theory* offers a good description of the electrostatic interactions between the charged membrane and the ions in the aqueous phase even though it strongly simplifies the real membrane-water interface.

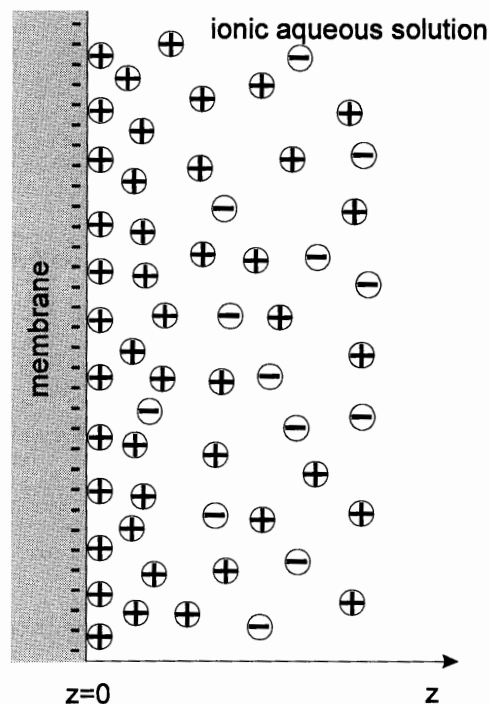


Figure 3. Membrane model used in the *Gouy-Chapman theory*.

The membrane-water interface is reduced to an infinite plane surface carrying a smeared surface charge which is in contact with the aqueous phase. The ions in the aqueous phase are treated as point charges, and ion-ion interactions, except those affected by the mean potential, are neglected. In Figure 3, the membrane model used for the *Gouy-Chapman theory* is shown.

An important feature of this model is the treatment of the three-dimensional membrane-water interface as a one-dimensional system. The *Gouy-Chapman theory* takes into account only interactions normal to the membrane surface, any interactions parallel to the membrane surface are neglected.

At an infinite distance from the surface the ions in the solution will not feel the repulsive or attractive force of the membrane surface charge, the electrical potential at an infinite distance is zero. But, as the surface is approached, the electric potential, ψ , gradually changes. It is assumed that the work required to bring an ion from the bulk of the solution to a point near the surface is entirely due to the electric potential. The distribution of ions in solution in the z -direction, normal to the surface, is then given by the following form of the *Boltzmann equation*,

$$N_i(z) = N_i(\infty) \exp\left(-\frac{z_i e \psi(z)}{kT}\right), \quad (1)$$

where $N_i(z)$ and $N_i(\infty)$ are respectively, the number of ions per unit volume of species i at a distance z from the surface, and the number of ions at an infinite distance from the surface and z_i denotes the valence of an ion i . The charge distribution in the aqueous phase and the electrical potential can be related to each other by the *Poisson equation* which takes, for this one-dimensional problem, the form

$$\frac{d^2 \psi(z)}{dz^2} = -\frac{\rho(z)}{\epsilon_r \epsilon_0}, \quad (2)$$

where ϵ_r is the uniform dielectric constant of the solution, ϵ_0 the permittivity of free space and $\rho(z)$ denotes the space charge density given by

$$\rho(z) = \sum_i z_i e N_i(z) \quad (3)$$

A combination of Eqs. 1, 2 and 3 yields the *Poisson-Boltzmann equation*

$$\frac{d^2\psi(z)}{dz^2} = -\frac{1}{\epsilon_r \epsilon_0} \sum_i z_i e N_i(\infty) \exp\left(-\frac{z_i e \psi(z)}{kT}\right). \quad (4)$$

The *Poisson-Boltzmann equation*, Eq. 4, is a nonlinear differential equation which has, in general, to be solved numerically. A first integration of Eq. 4 is analytically possible and results, together with the electroneutrality condition,

$$\sigma_m = -\int_0^{\infty} \rho(z) dz \quad (5)$$

in the *Gouy-Chapman equation*¹

$$\sigma_m = \left[2 \epsilon_r \epsilon_0 kT \sum_i N_i(\infty) \left\{ \exp\left(-\frac{z_i e \psi(0)}{kT}\right) - 1 \right\} \right]^{\frac{1}{2}} \quad (6)$$

¹ For a more detailed derivation see Appendix A or Aveyard and Haydon (1973).

σ_m denotes the surface charge density on the membrane surface and $\psi(0)$ the electric potential at the surface.

The *Gouy-Chapman equation* shows the relationship between the potential at the surface ($z = 0$), a quantity of great interest for the adsorption, the surface charge density and the ionic composition. To solve the *Poisson-Boltzmann equation* for any distance z from the membrane surface a linearization of the *Boltzmann factor*, instead of a numerical solution, is most often used. The *Poisson-Boltzmann equation* can be linearized for electric potentials small compared to $kT/e = 25$ mV using the approximation

$$\exp\left(-\frac{z_i e \psi(z)}{kT}\right) = 1 - \frac{z_i e \psi(z)}{kT} \quad (7)$$

which yields the linearized *Poisson-Boltzmann equation*

$$\frac{d^2 \psi(z)}{dz^2} = \frac{1}{\epsilon_r \epsilon_0} \sum_i z_i e N_i(\infty) \frac{z_i e \psi(z)}{kT} \quad (8)$$

The solution of this differential equation is easily obtained as

$$\psi(z) = \psi(0) e^{-Kz}, \quad (9)$$

where K is the inverse *Debye length*,

$$K = \left(\frac{e^2}{\epsilon_r \epsilon_0 kT} \sum_i z_i^2 N_i(\infty) \right)^{\frac{1}{2}} \quad (10)$$

The electric potential at the surface, $\psi(0)$, can be obtained from the *Gouy-Chapman equation*, Eq. 6.

The linearized *Poisson-Boltzmann equation*, Eq. 9, was used in all our calculations and we will refer to the potential obtained in this way as the linearized Gouy-Chapman potential.

1.2 The Discrete Charge Theory

Nelson and McQuarrie described, in 1975, an electrostatic model of the membrane-water interface which accounted for discreteness of membrane charge. They considered that the surface charges are discrete rather than uniform and calculated, on this basis, the electric potential distribution in the aqueous phase above the membrane surface. Their *discrete charge theory* is an extension of the successful *Gouy-Chapman theory* and differs from the *Gouy-Chapman theory* in just two points: (1) The membrane surface charge density is modeled as a two-dimensional array of discrete charges instead of a smeared surface charge and (2) the theory allows an embedding of discrete charges below the membrane surface.

The model used for the *discrete charge theory* is shown in Figure 4. The membrane surface is located at the $z = 0$ plane and an array of charges are located at a distance c behind the membrane surface. The charges in the model of Nelson and McQuarrie are arranged in a periodic manner, on a square lattice. Regions 1 and 2 correspond to the membrane core and membrane surface layer, region 3 to the ionic aqueous solution. Dividing the membrane into two regions

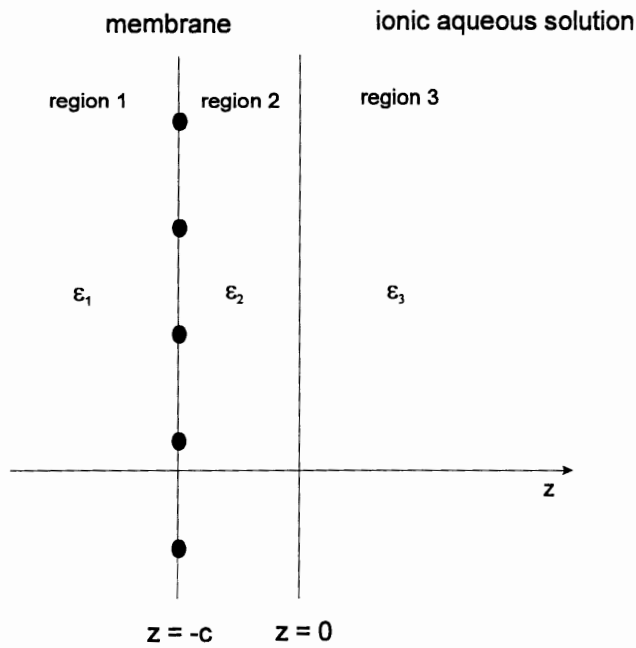


Figure 4. Membrane model used in the *discrete charge theory*.

takes into account the dielectric inhomogeneity of the membrane. The dielectric constant of the aqueous phase is assumed not to change significantly as a function of distance from the membrane surface.

In the following paragraphs the important elements in the derivation of this model are given. For a more detailed derivation the reader should refer to Nelson and McQuarrie (1975).

The electric potential in region 1 and region 2 satisfy *Laplace's equation*,

$$\Delta\psi_1 = \Delta\psi_2 = 0 \quad (11)$$

In region 3 the electric potential is described by the *Poisson equation*

$$\Delta\psi_3(\vec{r}) = -\frac{\rho(\vec{r})}{\epsilon_3 \epsilon_0} \quad (12)$$

The electric potentials in all regions are invariant under a lattice transformation as the charges are arranged in a periodic manner and can, therefore, be expanded in a Fourier series of the form

$$\psi(\vec{r}) = \sum_{\vec{G}} f_{\vec{G}}(z) e^{i\vec{G}\vec{r}} \quad (13)$$

where G is a reciprocal lattice vector, two-dimensional in our case. It is given by

$$\vec{G} = h\vec{A} + k\vec{B}, \quad (14)$$

where h and k are integers (Miller indices). For the case of a two-dimensional square lattice with lattice constant a , the reciprocal lattice vectors are given by

$$\vec{A} = \frac{2\pi}{a} \hat{x} \quad \vec{B} = \frac{2\pi}{a} \hat{y} \quad (15)$$

Substituting Eq. 13 into Eq. 12 the electric potential in region 1 and 2 can be written as

$$\psi_1(\vec{r}) = \sum_{\vec{G}} E_{\vec{G}} e^{i\vec{G}\vec{r}} e^{+Gz} \quad (16)$$

and

$$\psi_2(\vec{r}) = \sum_{\vec{G}} (C_{\vec{G}} e^{i\vec{G}\vec{r}} e^{-Gz} + D_{\vec{G}} e^{i\vec{G}\vec{r}} e^{+Gz}) \quad (17)$$

The electric potential in region 3 obeys the Poisson equation, Eq. 13, which together with the space charge density

$$\rho(\vec{r}) = \sum_i z_i e N_i(\vec{r}) \quad (18)$$

and the *Boltzmann equation*

$$N_i(\vec{r}) = N_i(\infty) \exp\left(-\frac{z_i e \psi_3(\vec{r})}{kT}\right) \quad (19)$$

results in the following nonlinear differential equation

$$\begin{aligned} & \sum_{\vec{G}} \left[\frac{\partial^2}{\partial z^2} f_{\vec{G}}(z) e^{i\vec{G}\vec{r}} - (G_x^2 + G_y^2) f_{\vec{G}}(z) e^{i\vec{G}\vec{r}} \right] \\ &= - \sum_i \frac{z_i e N_i(\infty)}{\epsilon_r \epsilon_0} \exp\left(-\frac{z_i e}{kT} \sum_{\vec{G}} f_{\vec{G}}(z) e^{i\vec{G}\vec{r}}\right) \end{aligned} \quad (20)$$

This nonlinear differential equation can not be solved analytically. Nelson and McQuarrie assumed in their derivation that the *Debye-Hückel theory* can be applied to region 3. This is equivalent to the assumption that the *Boltzmann factor* can be linearized as

$$\exp\left(-\frac{z_i e}{kT} \sum_{\vec{G}} f_{\vec{G}}(z) e^{i\vec{G}\vec{r}}\right) = 1 - \frac{z_i e}{kT} \sum_{\vec{G}} f_{\vec{G}}(z) e^{i\vec{G}\vec{r}} \quad (21)$$

Equation 20 simplifies then into

$$\frac{\partial^2 f_{\bar{G}}}{\partial z^2} - (G^2 + K^2)f_{\bar{G}} = 0 \quad (22)$$

where K is the inverse *Debye length*, already defined in Eq. 10

$$K = \left(\frac{e^2}{\epsilon_r \epsilon_0 kT} \sum_i z_i^2 N_i(\infty) \right)^{\frac{1}{2}} \quad (10)$$

Using this approximation the electric potential in region 3 can be written as

$$\psi_3(\bar{r}) = \sum_{\bar{G}} A_{\bar{G}} e^{i\bar{G}\bar{r}} e^{-(G^2+K^2)^{\frac{1}{2}}z} \quad (23)$$

The constant $A_{\bar{G}}$ in Eq. 23 can be determined from the boundary conditions,

$$\psi_1(-c) = \psi_2(-c) \quad (24)$$

$$\epsilon_1 \frac{\partial \psi_1}{\partial z} \Big|_{z=-c} = \epsilon_2 \frac{\partial \psi_2}{\partial z} \Big|_{z=-c} + \frac{\sigma}{\epsilon_0} \quad (25)$$

$$\psi_2(0) = \psi_3(0) \quad (26)$$

$$\epsilon_2 \frac{\partial \psi_2}{\partial z} \Big|_{z=0} = \epsilon_3 \frac{\partial \psi_3}{\partial z} \Big|_{z=0} \quad (27)$$

Since the charges are arranged in a periodic manner, the surface charge density σ in Eq. 25 can be expanded into a Fourier series

$$\sigma = \sum_{\vec{G}} \sigma_{\vec{G}} e^{i\vec{G}\vec{r}} \quad (28)$$

and after some tedious algebra, the following expression for $A_{\vec{G}}$ can be obtained

$$A_{\vec{G}} = \frac{\sigma_{\vec{G}}}{\epsilon_0} \cdot \frac{1}{\epsilon_1 G \cosh Gc + (\epsilon_3 \epsilon_1 / \epsilon_2) (G^2 + K^2)^{\frac{1}{2}} \sinh Gc + \epsilon_2 G \sinh Gc + \epsilon_3 (G^2 + K^2)^{\frac{1}{2}} \cosh Gc} \quad (29)$$

The factor $\sigma_{\vec{G}}$ for a simple square lattice with one ion of charge q located at each lattice point, is given by²

$$\sigma_{\vec{G}} = q/a^2 \quad (30)$$

Finally, a combination of Eqs. 23, 29 and 30 and the simplifying assumption that the membrane region has a uniform dielectric constant, $\epsilon_1 = \epsilon_2$, results in

$$\psi_3(\vec{r}) = \frac{q}{2\pi a \epsilon_0} \sum_{h,k} \frac{1}{\exp(\sqrt{h^2 + k^2} \cdot 2\pi c/a)} \cdot \frac{1}{\epsilon_1 (h^2 + k^2) + \epsilon_3 \sqrt{h^2 + k^2 + m^2}} \cos(2\pi h x/a + 2\pi k y/a) \cdot \exp(-\sqrt{h^2 + k^2 + m^2} \cdot 2\pi z/a) \quad (31)$$

where $m = Ka/2\pi$.

² For a detailed derivation see Nelson and McQuarrie (1975).

This expression, Eq. 31, was used in all our calculations. Below we refer to this electric potential as the discrete charge potential.

1.3 The Boltzmann Factor

The *Boltzmann factor*, $Bf_{z_i}(\bar{r})$, for an ion of valence z_i is defined as

$$Bf_{z_i}(\bar{r}) = \exp(-ez_i \psi(\bar{r})/kT). \quad (32)$$

The *Boltzmann factor* relates bulk and interfacial concentrations of ions and plays an important role in ion adsorption to biological membranes.

2 Electrical Potential and Ion Concentration Distribution in the Vicinity of the Charged Membrane Surface

2.1 Computations

The linearized Gouy-Chapman potential, Eq. 9, the discrete charge potential, Eq. 31, and the respective Boltzmann factors were calculated using a Visual Basic computer program. The calculations were done on IBM compatible 486/33 computer.

The important elements of this program are:

- (1) Determination of the ionic composition of the aqueous solution and the calculation of the Debye length.
- (2) Determination of the Gouy-Chapman potential at the membrane surface from Eq. 6 for given surface charge density and ionic composition of aqueous solution.
- (3) Calculation of the linearized Gouy-Chapman potential according to Eq. 9.

- (4) Calculation of the discrete charge potential according to Eq. 31.
- (5) Calculation of the Boltzmann factor, Eq. 32, for hexavalent positively charged Ruthenium Red ions for two cases: (i) the discrete charge model and (ii) the smeared charge electrostatic model.

The computations in steps (1) to (3) and (5) are straightforward. By performing steps (1) to (3), the linearized Gouy-Chapman potential was obtained for given experimental conditions such as surface charge density and ionic composition of the aqueous solution. Boltzmann factors in step (5) were calculated according to Eq. 32. The calculations of the discrete charge potential were performed by summations over h and k from -49 to $+49$. This corresponds to a square array of 99×99 discrete charges on the membrane surface. The relatively large array was necessary to avoid oscillations in the potential and to obtain correct results at distances close to the membrane surface.³ We have taken the advantage of the symmetry of the square lattice so that it was necessary to calculate potentials only for a quarter of the square unit cell ($0 \leq x \leq a/2$ and $0 \leq y \leq a/2$). The potential in this quarter cell was obtained for 100 equidistant grid points to achieve a good spacial resolution of the potential and to make possible accurate averaging of both the potential and the Boltzmann factor. Potential profiles for the whole array or an arbitrary section of the array can then be easily obtained

³ Oscillations in the potential occur due to the Fourier series expansion of the potential. The accuracy of the expansion increases with the size of the array and high orders of Fourier series expansion are particularly important for calculations of the potentials close to the membrane surface since the potential rapidly changes there.

by shifting and mirroring this quarter cell. This approach speeded considerably the computations (on a scale of minutes).

2.2 Results

In all the calculations we assumed a dielectric constant for the aqueous phase of $\epsilon_3 = 78.5$ and considered the membrane as a homogenous region with a dielectric constant, $\epsilon_1 = \epsilon_2 = 3$. The ionic composition was 0.03 M monovalent salt, citrate/borate/phosphate (2mM/2mM/0.5mM) buffer, 1 mM Ruthenium Red, pH 7, unless stated differently.

Figure 5 and Figure 6 show spacial distributions of the electric potential and ion concentration potential profiles for the discrete charge model. These profiles were calculated for three different distances, z , from the membrane surface, $z = 1\text{\AA}$, $z = 2\text{\AA}$ and $z = 5\text{\AA}$. Due to the screening effect of the counterions, the magnitude of the potential decreases very rapidly with the distance from the membrane surface. At the membrane surface, the potential distribution looks like a set of delta functions. Due to the effective screening only very small humps in the potential profile can be seen at a distance 5\AA from the membrane surface.

Concentration profiles, as can be seen in Figure 6 are very different. The extreme sharpness of the ion concentration peaks is because the ion concentration depends exponentially on the electric potential (recall the Boltzmann factor). The computed results illustrate the potentially important role of membrane discrete charges on the ion distribution in the vicinity of the membrane surface.

The dependence of the Gouy-Chapman and the discrete charge potential on the distance z from the membrane surface is illustrated in Figure 7. In this figure we compare electric potentials at several locations within the square unit cell of a charge array. The “minimum” potential corresponds to the center of the square unit cell whereas the “maximum” potential to the region above the discrete charge. The solid curves depict the “average” potential obtained by averaging the electric potential distribution over the unit cell. The ionic composition in Figure 7(a) and (b) differs only by the absence and the presence of Ruthenium Red (1mM). As can be seen in Figure 7(a) the “average” potential obtained from the discrete charge model and the Gouy-Chapman potential obtained from the smeared charge model are nearly identical. The breakdown of the Nelson and McQuarrie model is seen in Figure 7(b) which shows a discrepancy between the “average” and the Gouy-Chapman potential in the presence of a multiply charged counterion. This is because of the inapplicability of the linearization of the Boltzmann factor (see Eq. 21).

Figure 8 shows that “minimum” (Figure 8b) and “maximum” (Figure 8a) potentials converge with increasing embedding depth of the membrane charges to the “average” potential. The average potential did not change with embedding depth. In addition, the embedding of membrane charges causes smoothing of spacial variation of electric potential. The differences between electric potential computed for the discrete charge and the smeared charge distribution progressively decrease with the increase of the embedding depth.

A plot of the electric potential as a function of surface charge density is given in Figure 9 (the potential is calculated at a distance $z = 0.1$ nm from the membrane surface and for charges at the membrane surface). This plot shows that the discrepancy between the smeared charge and discrete charge model

increases with increasing surface charge density: the “average” negative potential increases rapidly with the increasing surface charge density in a linear fashion. In contrast the increase in the Gouy-Chapman potential with the surface charge density is less rapid.

The Boltzmann factors as a function of distance z from the membrane surface are shown in Figure 10. The differences between the Boltzmann factors obtained for the discrete charge model and the Gouy-Chapman model are enormous but their occurrence is probably to a great extent caused by the invalid approximation of linearization of the Boltzmann factor, Eq. 21, done in the discrete charge model. Evidence of the inconsistency of the linearization of the Boltzmann factor can be seen when comparing the plot of the linearized Boltzmann factor, designated as “linearized discrete charge model”, with the non-linearized Boltzmann factor obtained with the discrete charge model. If the linearization of the Boltzmann factor according to Eq. 21 is valid, the Boltzmann factor obtained for the discrete charge potential should be approximately the same as that for the linearized and the non-linearized Boltzmann factor. The great gap between the non-linearized and the linearized Boltzmann factor shows the breakdown of the linearization of the Boltzmann factor in the discrete charge theory.

The embedding of the charges in the membrane causes a decrease in the Boltzmann factor obtained for the discrete charge theory, as can be seen in Figure 11(a) and (b) whereas the embedding cannot be calculated with the current version of the Gouy-Chapman theory. The gap between Boltzmann factors increases with the increasing surface charge density very rapidly. According to Voelker (1994) the Boltzmann factor obtained in experiments with hexavalent Ruthenium Red was found to be smaller than the Boltzmann

factor obtained from the Gouy-Chapman theory. This discrepancy indicates the inapplicability of the current version of the discrete charge theory. We conclude that the discrete charge theory cannot be used as a tool to predict the effect of discrete charges, the reason is that the approximation on which the current theory has been constructed for nearly all real experimental conditions breaks down.

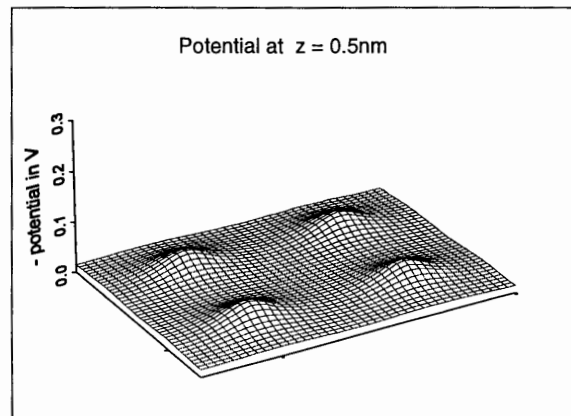
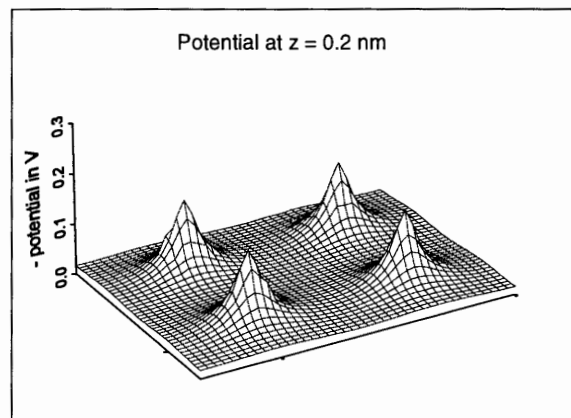
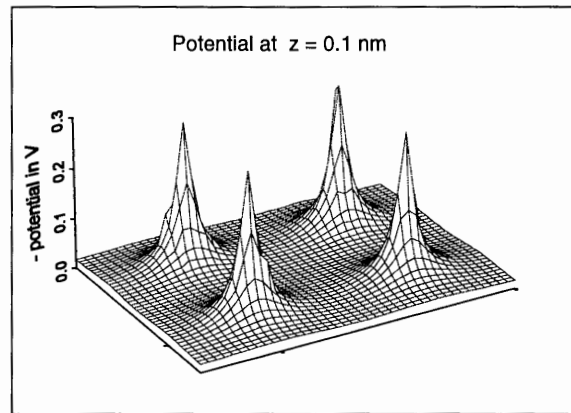


Figure 5. Potential profiles for various distances z from the membrane surface; the charges are located directly at the membrane surface ($c = 0$), surface charge density = 0.126 e/nm^2 (corresponds to a lattice constant $a = 2.8 \text{ nm}$), and Ruthenium concentration = 1 mM .

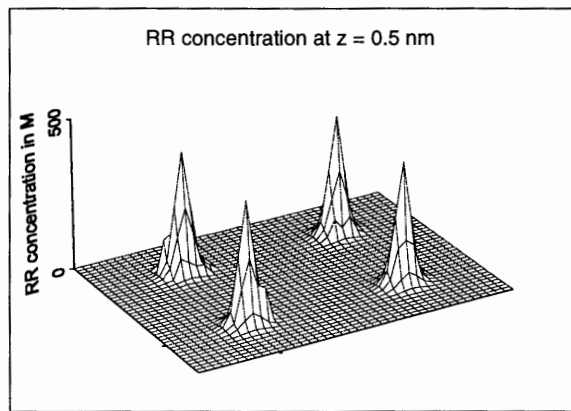
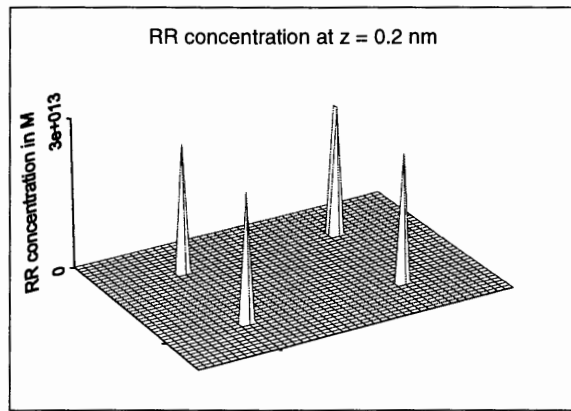
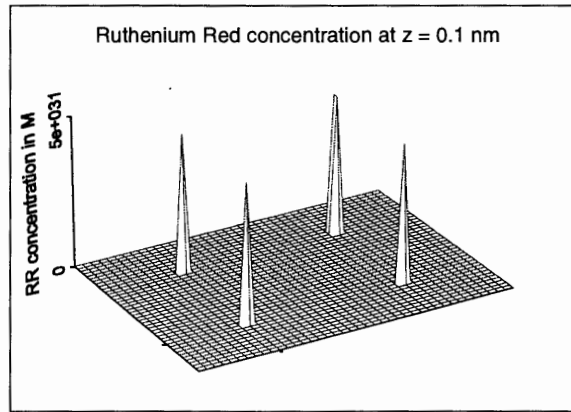


Figure 6. Concentration profiles for various distances z from the membrane surface; parameters are the same as in Figure 5.

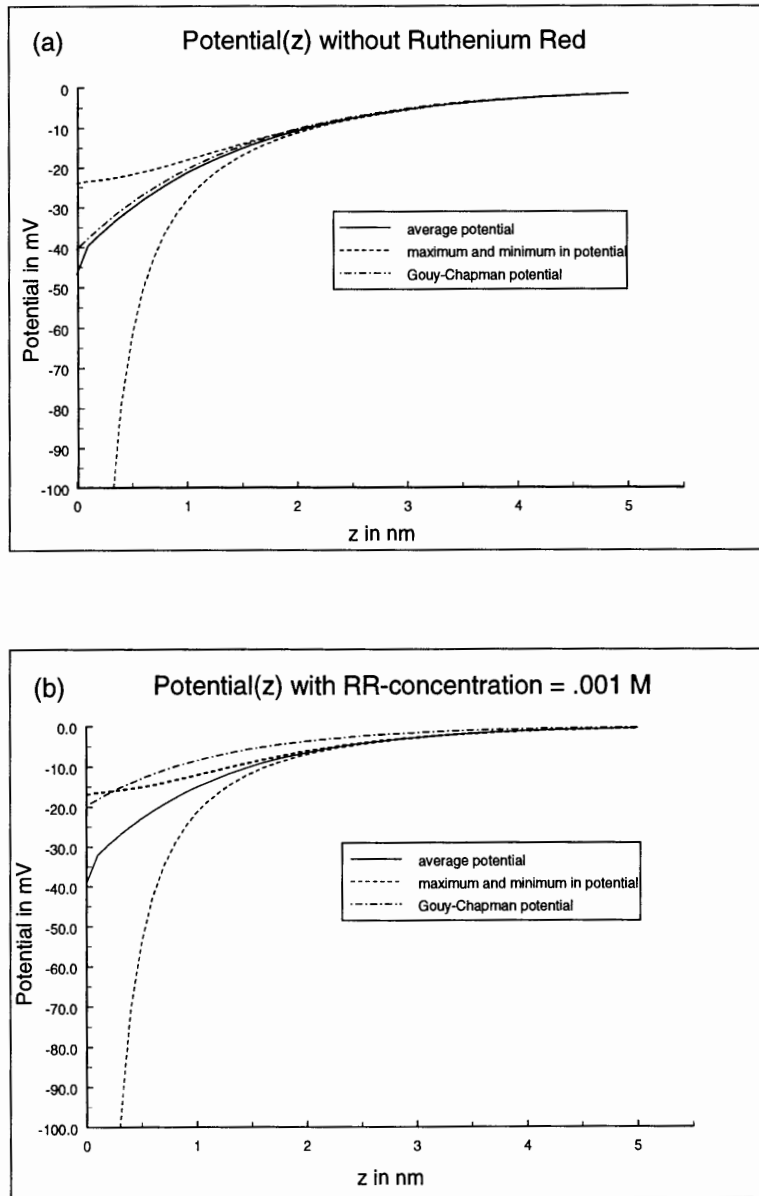


Figure 7. The potential as a function of distance from the membrane surface; the charges are directly located at the membrane surface ($c = 0$), and the surface charge density is 0.126 e/nm^2 (corresponds to a lattice constant $a = 2.8 \text{ nm}$). The graph (a) shows the potential without Ruthenium Red in the aqueous solution, the graph (b) the potential with a 1 mM Ruthenium Red concentration.

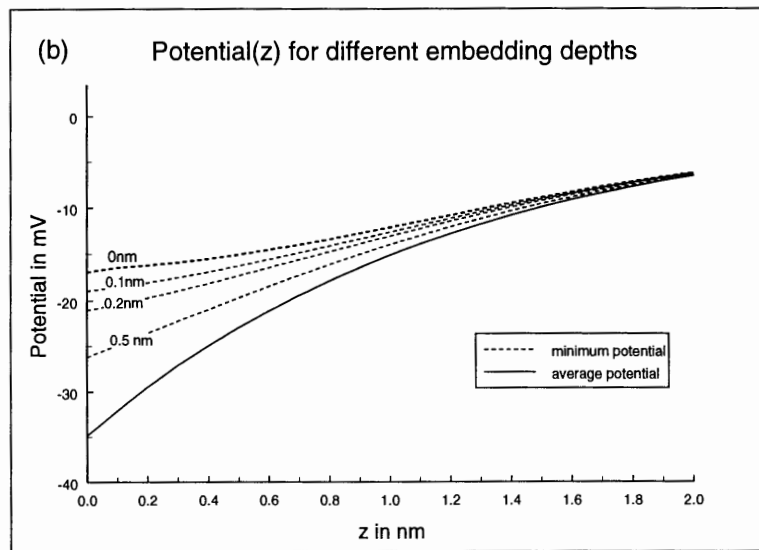
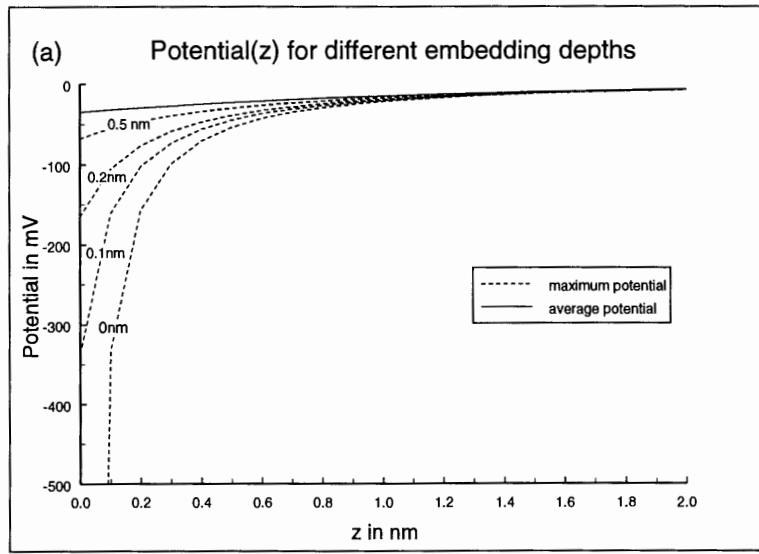


Figure 8. The potential as a function of the distance z from the membrane; for surface charge density 0.126 e/nm^2 . The potentials, (a) maximum potential, (b) minimum potential, are calculated for the embedding depths $c = 0 \text{ nm}$, $c = 0.1 \text{ nm}$, $c = 0.2 \text{ nm}$ and $c = 0.5 \text{ nm}$.

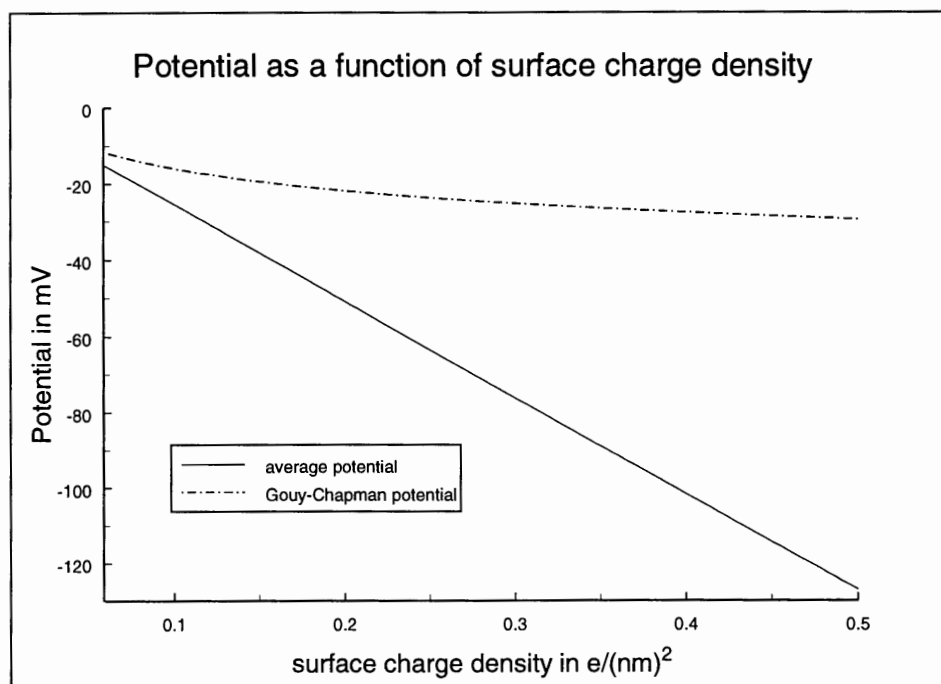


Figure 9. The electric potential as a function of surface charge density. Charges are assumed to be located directly at the membrane surface ($c = 0$), the potential was calculated for distance $z = 0.1$ nm from the membrane surface.

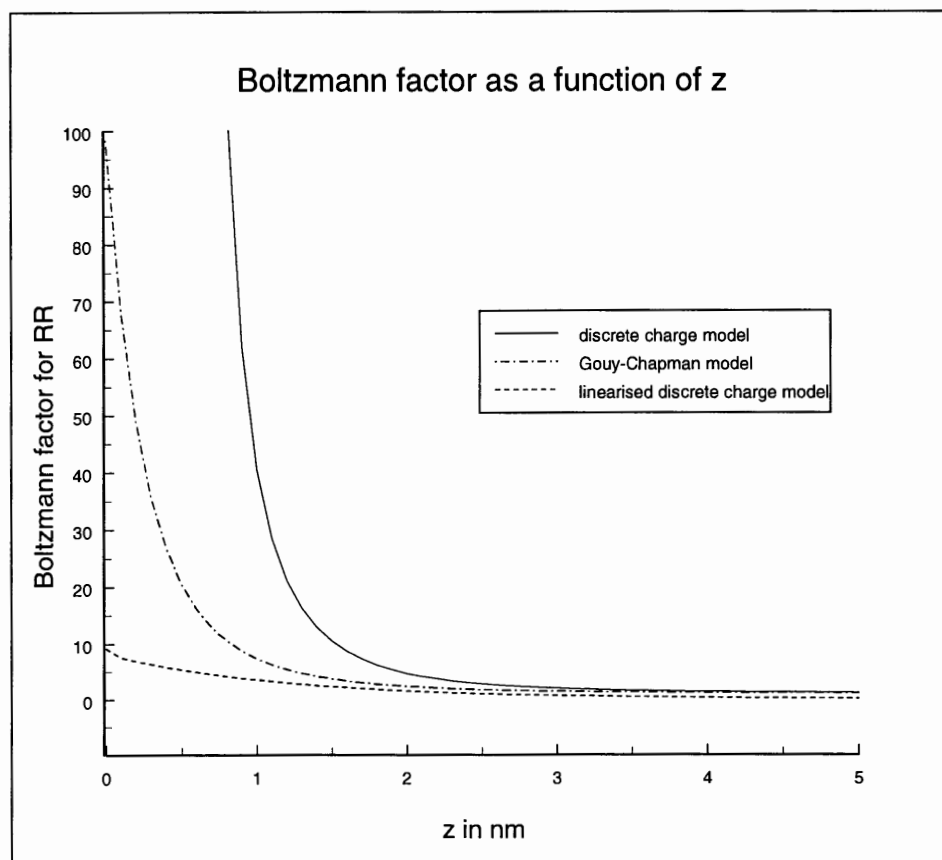


Figure 10. The Boltzmann factor as a function of distance z from the membrane surface. Charges are assumed to be located directly at the membrane surface ($c = 0$), the surface charge density 0.126 e/nm^2 .

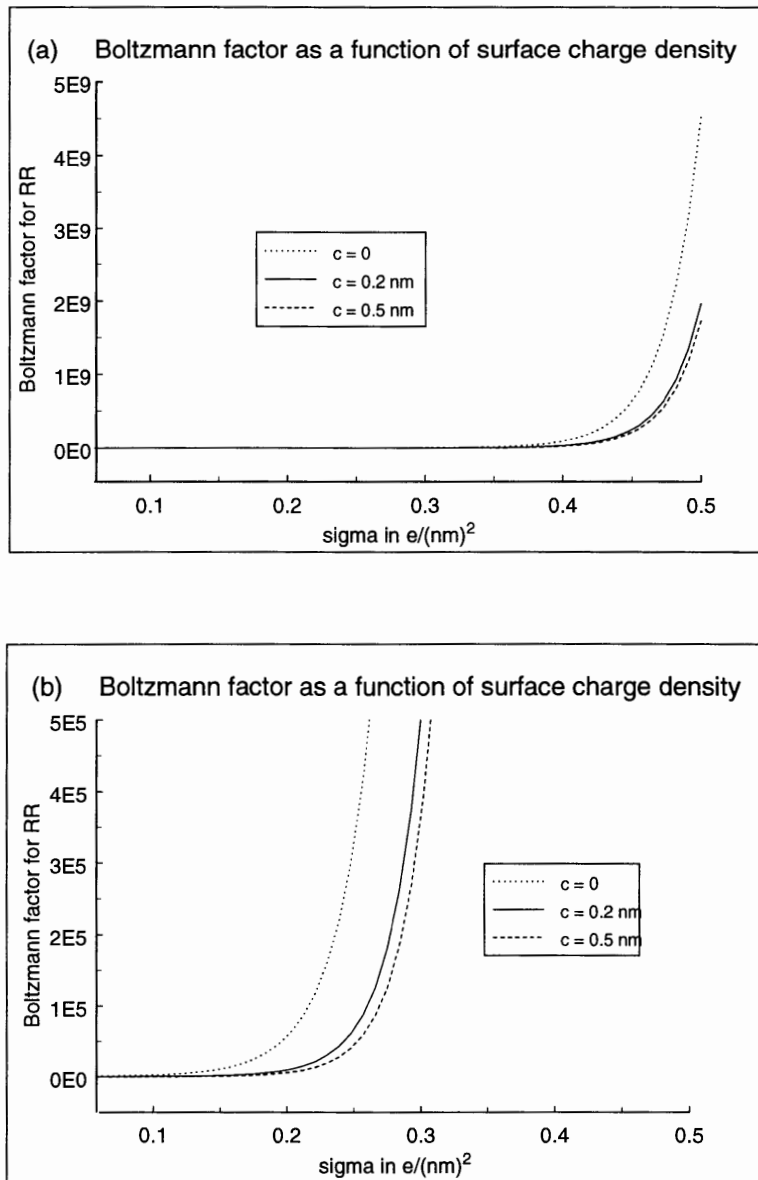


Figure 11. The dependence of Boltzmann factor on the surface charge density; (a) the Boltzmann factor for the discrete charge model, (b) an enlarged part of (a). The Boltzmann factor was calculated at a distance $z = 5 \text{ \AA}$ from the membrane surface.

Part II

Distribution of 2,4,6-Trichlorophenol in a Membrane Model System

3 Introduction

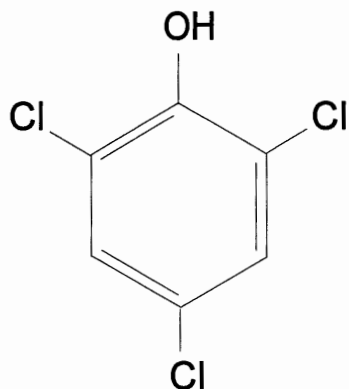


Figure 12.
Molecular structure of
2,4,6-Trichlorophenol

In this research project we determine the distribution of 2,4,6-Trichlorophenol (2,4,6-TrCP) in the octanol-water system which is used as a model system for biological membranes. The octanol-water system - a detailed description of which is given in section 4.1.2 - is widely used for modeling adsorption and partitioning of hydrophobic compounds, such as 2,4,6-TrCP.

The chemical structure of 2,4,6-TrCP is shown in Figure 12. Chlorophenols exist either in an un-ionized or an ionized form depending on the acidity of the aqueous environment. The dissociation constants of chlorophenols are typically 10^{-3} - 10^{-9} which corresponds to pKa values of 3-9. The pKa value of 2,4,6-TrCP is 6.1 (Schellenberg et al., 1984).

The distribution of un-ionized species of chlorophenols in the octanol-water system has been studied earlier (Schellenberg et al., 1984; Callahan et al., 1979; Xie et al., 1984 and Leo et al., 1971), however data for the distribution of the ionized species are not available. Furthermore, the suitability of the octanol-water system as a model for biomembranes has not been demonstrated for the ionized species. In the present work we report results on the distribution of 2,4,6-TrCP for both ionized and un-ionized species and compare our results with those obtained from adsorption studies done on lipid membranes under the same experimental conditions.

The study and the development of membrane adsorption models for 2,4,6-Trichlorophenol as well as for other chlorophenols is of great interest as the chlorophenols are strong biocides and are present in the environment due to their wide industrial and agricultural use. Their relatively high toxicity raises questions concerning the environmental impact of these materials. The behavior in which toxic compounds move and are distributed in the environment is complex. This project contributes to the development of understanding of distribution of 2,4,6-TrCP in the environment by obtaining data on the distribution of this compound in a model, the octanol-water system.

Below we present information on the occurrence of chlorophenols in the environment and on their toxicity.

The most widely used chlorophenol was pentachlorophenol (PCP). This chemical was extensively used as an industrial biocide and as an agricultural pesticide (Beynon et al., 1981).

Tetrachlorophenols (TeCP's) and trichlorophenols (TrCP's) are also found in the environment, often as degradation products of PCP. The compound of our present interest, 2,4,6-TrCP, has been used in the past as a germicide, bactericide, wood and glue preservative, and as an antimildew agent (Sittig, 1985). Various TeCP's and other TrCP's, including 2,4,6-TrCP are byproducts of chlorobleaching of pulp and therefore present in the wastewater from wood pulp bleaching mills (Paasivirta et al., 1992). Breakdown processes of PCP through sunlight (Mikesell and Boyd, 1986) and anaerobic biodegradation (Nicholson et al., 1992) are major sources of all the different chlorinated phenols even if they are not directly used in industry or agriculture.

The production of PCP and therefore the introduction of all chlorophenols into the environment started in the 1930's and reached by 1981 a

worldwide production of 50 000 metric tones, as estimated by Beynon and coworkers (Beynon et al., 1981). The mass production and extensive use of PCP has been discontinued and is today restricted in many countries such as Sweden, USA, Japan and Germany. Even though the use of PCP has been restricted nowadays, the extensive and wide use in the past has had an enormous impact on environment and chlorophenols are still major pollutants.

Wild et al. (1992) estimated that about 90% of the environmental burden of PCP is associated with the soil, water follows as the next significant sink. Humans are also exposed to PCP and other chlorophenols. The primary exposure route of chlorophenols is most likely via ingestion of contaminated food and water, inhalation of vaporized chlorophenols and skin absorption by direct contact with laundry products, wooden goods, leather, paper and textiles. The main route of PCP uptake by the general population is by ingestion of contaminated food, whereas uptake due to inhalation of vaporized PCP plays an important role for occupationally exposed individuals. Geyer et al. (1987) reported a daily PCP ingestion of an average adult to be about 19 μg . The PCP body burden of humans ranges, according to literature values, between 533 μg and 673 μg and PCP is mainly concentrated in the liver and the brain (Geyer et al., 1987; Hattemeyer-Frey and Travis, 1989; and Wild and Jones; 1992). In another study by Mussalo-Rauhamaa et al. (1989) the concentrations of 2,4,6-TrCP, 2,3,4,6-TeCP and PCP in the tissues of people from Finland were studied. The TrCP and TeCP concentrations were found to be significantly lower than PCP concentrations. 2,4,6-TrCP was not detectable. The presence of 2,4,6-TrCP at a level of 12 $\mu\text{g/l}$ indicates an additional lifetime cancer risk of 1 in 100,000 (Sittig, 1985).

Studies of human exposure to chlorophenols can give only a rough idea of the factors and consequences involved in potential human exposure. Knowledge of the presence and fate of chlorophenols in sediments, soil, air, water, and organisms is therefore essential to relate their persistence and movement in the environment to potential human exposure. It is not possible to evaluate all polluted sites and to account for all conditions associated with the presence of chlorophenols in the environment. Therefore models, such as the octanol-water system, that enable us to predict chlorophenol concentrations under various conditions are essential.

On the cellular level, chlorophenols are found to be toxic due to their action as uncouplers of oxidative phosphorylation.⁴ ATP synthesis is strongly coupled to the H⁺-gradient across the inner mitochondrial membrane. A lowering of this H⁺-gradient due to the activity of chlorophenols, as they transport protons across the membrane, disrupts the coupling between this H⁺-gradient and the ATP synthesis. If the uncoupling effect is strong, not enough ATP can be produced to supply the energy for all cell functions and the cell will die.

The ability of chlorophenols to act as carriers of H⁺-ions can be described by two different mechanisms: A neutral chlorophenol (HA) permeates the membrane and releases a H⁺-ion at the more basic matrix side of the membrane, the ionized chlorophenol (A⁻) diffuses back to the more acidic side, picks up another H⁺-ion to release it again on the more basic side (Terada 1990). Another alternative to the back diffusion is the transmembrane flow of AHA⁻ dimers (Smejtek et al., 1976). Both mechanisms show that the uncoupling activity depends strongly on the lipophilicity of the chlorophenol,

⁴ 2,4,6-TrCP is also a carcinogen (Sittig, 1985).

the greater the adsorption and the greater the rate of permeation through the membrane the stronger is the uncoupling effect. The weak acidity of chlorophenols, their ability to exist as phenolate ions, is necessary to make the transfer of protons possible.

Adsorption studies of chlorophenols to biological membranes serve two different purposes: (1) Adsorption studies of chlorophenols to biological membranes provide a better understanding of their toxicity and (2) adsorption to biological membranes plays an important role in estimating the concentration of the chlorophenols in soils, sediments and organisms as all these materials contain membranes and membrane fragments.⁵

The adsorption or partitioning of the chlorophenols from water into biological cells or organic components of sediments and soils (Schellenberg et al. 1984, Lagas 1988) has been extensively modeled by the transfer of these chemicals from water to octanol. We use therefore, the octanol-water system as a model system in our experiments. For the description of the partitioning in the octanol-water system, the octanol-water partition coefficient is defined by

$$P_{ow} = \frac{[X]_o}{[X]_w},$$

where $[X]_o$ is the concentration of the compound of interest in octanol and $[X]_w$ is its concentration in water. The octanol-water partition coefficient is a widely used tool and has numerous applications in addition to predicting the presence of toxic compounds in the environment.

⁵Soil and sediments contain biological membranes due to the presence of live and dead cells and cell fragments (Wang, Goving and Dobbs 1993).

The octanol-water partition coefficient can be obtained by a direct measurement and to a certain degree by calculation from known physico-chemical properties of a chemical. Approaches to obtain partition coefficient are many, some of them are combining experimental measurements and quantum-mechanical calculations.⁶

In our research we used the shake flask method: the examined compound X was injected into a two-phase system consisting of known volumes of octanol and water. After shaking the solution to reach the equilibrium distribution, the two phases were separated and the concentrations in each phase determined. This procedure belongs to a class of direct methods of measurements of P_{ow} . A more detailed description of this method is given in chapter 6.

The usefulness of octanol-water partition coefficients rests on the assumed similarity of the energetics of transfer of hydrophobic chemicals from water into octanol to that from water into biological membranes. We question this similarity for ionized chlorophenols since a significant discrepancy between the partitioning in the octanol-water system and adsorption to phospholipid vesicles was found for PCP. Smejtek and Wang (1993) compared partitioning of PCP in the octanol-water system with the adsorption to phospholipid vesicles and found substantial differences for $pH > pK_a$. The energetics of transfer of

⁶The different ways of determining octanol-water partition coefficients include several different experimental methods and theoretical approaches which use the physico-chemical properties of the partitioning species to predict the octanol-water partition coefficient. Other methods use: reversed-phase high-performance liquid chromatography (RP-HPLC) (Klein et al., 1988), calculation of P_{ow} from water solubility (Miller et al., 1985), from chemical structure which include factors like shape, molecular volume, total molecular surface area (TSA) and total molecular volume (TMV) of a compound (Bruijin and Hermens 1990, Sabijic et al., 1993). A critical review of the measurements of octanol-water partition coefficients is given by Chessells et al. (1991).

the ionized species of PCP in octanol-water and membrane-water system was found to be not comparable: the octanol-water partition coefficient of the ionized species of PCP was several orders of magnitude smaller than the membrane-water partition coefficient.

The goal of our study was to measure the octanol-water partition coefficient of 2,4,6-TrCP as a function of pH in order to obtain partition coefficients for the un-ionized as well as ionized species of 2,4,6-TrCP and to compare the obtained data with results of Blochel (1992) who measured adsorption of ionized chlorophenols to lipid membranes under the same conditions. The objective was to test the applicability of the octanol-water partition coefficient for the phenolate of 2,4,6-TrCP to membrane adsorption.

4. Theory

4.1 Partition of Un-ionized and Ionized Molecules Between Water and a Medium of Low Polarity

The distribution of 2,4,6-TrCP between octanol and an aqueous phase as a function of pH was measured. It is important to recognize that the partitioning of 2,4,6-TrCP between octanol and water is not an ideal partitioning process⁷. Octanol and water are partially miscible and therefore the two phases are not ideal. In addition, 2,4,6-TrCP exists in the aqueous phase in two forms: ionized and un-ionized. The ionization is pH dependent and each species is exhibiting totally different partitioning behavior. Buffer components, which are expected to be strongly coupled to the partitioning of the ionized species, also contribute to the non-ideal behavior of the system.

We present first the concepts of ideal partitioning (Gerthsen et al., 1986; Herrmann, 1993) since they provide the foundation for the understanding of distribution of ionized and un-ionized species between octanol and aqueous phase. A short overview of thermodynamics given in section 4.1.1 provides the necessary insight into the basic properties of an ideal partitioning system. In

⁷ Ideal partitioning assumes two homogenous extended bulk phases, ideal gas behavior of the solutes and independent partitioning of each species in case of the presence of several compounds.

4.1.2 we describe the octanol-water system. The definitions of the various partition parameters for membrane-water system follow in 4.1.3.

4.1.1 Ideal Partitioning

The distribution of several substances between two phases takes place in such a way so that the entropy of the system is maximized. Using the fact that pressure and temperature are constant during the partitioning process, the maximization of the entropy is equivalent to minimization of the free energy, G . The free energy G is defined by

$$G(T, p, n) = U + pV - TS, \quad (33)$$

where T is the temperature, p the pressure, n the number of particles, U the internal energy and S the entropy.

First we consider a system with just one solute. It is assumed that each species behaves like an ideal gas and its behavior is independent of the concentration of the other compounds present in the system. This concept can be easily generalized to a system with several components.

The differential of the free energy is given by

$$dG = \frac{\partial G(T, p, n)}{\partial T} dT + \frac{\partial G(T, p, n)}{\partial p} dp + \frac{\partial G(T, p, n)}{\partial n} dn \quad (34)$$

From the definition of free energy follows that

$$\begin{aligned}
dG &= d(U + pV - TS) \\
&= TdS - pdV + \mu dn + pdV + Vdp - TdS - SdT \\
&= Vdp - SdT + \mu dn
\end{aligned}
\tag{35}$$

At constant temperature and pressure the first two terms in Eq. 34 are zero since $dT = 0$ and $dp = 0$. Then the change of free energy is given by

$$dG = \mu dn \tag{36}$$

From the comparison of Eqs. 34 and 35 follows the definition of the chemical potential, μ .

$$\mu(T, p, n) = \frac{\partial G(T, p, n)}{\partial n} \tag{37}$$

Using one of Maxwell's relations

$$\frac{\partial^2 G(T, p, n)}{\partial p \partial n} = \frac{\partial V(T, p, n)}{\partial n} = \frac{\partial \mu(T, p, n)}{\partial p} \tag{38}$$

and applying the ideal gas law

$$pV = nRT \tag{39}$$

we obtain a differential equation relating changes in chemical potential to changes in pressure.

$$d\mu(T, p, n) = \frac{RT}{p} dp \quad (40)$$

Integration of Eq. 40, assuming that the standard chemical potential, μ_0^* , corresponds to the pressure, p_0 , yields,

$$\mu = \mu_0^* + RT \ln \frac{p}{p_0} \quad (41)$$

This relationship between the pressure and the chemical potential is not very useful for the description of transfer of molecules between two dense media. However the pressure can be easily related to the molar concentration, c , of a partitioning compound by applying the ideal gas law, Eq. 39,

$$p = \frac{n}{V} RT = cRT \quad (42)$$

This results in

$$\mu = \mu_0^* + RT \ln \left(\frac{c}{c_0} \right) = \mu_0^* - RT \ln c_0 + RT \ln c = \mu_0 + RT \ln c \quad (43)$$

After determining the relationship between the chemical potential and the concentration we return to the minimization of the free energy. The change in free energy of the whole system is given by the sum of the changes in free energy of the two phases. Phase one is designated by the single prime and

phase two by the double prime notation and, in the last step, the conservation of particles $dn' = -dn''$ is used:

$$dG = dG' + dG'' = \mu' dn' + \mu'' dn'' = (\mu' - \mu'') dn' \quad (44)$$

The equilibrium condition, $dG = 0$, yields

$$\frac{(\mu'_0 - \mu''_0)}{RT} = \ln c'' - \ln c' = \ln \frac{c''}{c'} \quad (45)$$

The molar partition coefficient P_c is therefore related to a characteristic change of free energy, ΔG_0 , the so called free energy of transfer

$$P_c = \frac{c''}{c'} = e^{(\mu'_0 - \mu''_0)/RT} = e^{-\Delta G_0/RT} \quad (46)$$

Equation 46 describes the connection between the partition coefficient P_c , an experimentally measurable quantity, and the free energy of transfer - the energy needed to transfer one mole of a compound from one phase to the other phase. For an ideal partitioning system the characteristic free energy of transfer can therefore be determined experimentally. Since the partition coefficients are commonly given as decadic logarithms, we obtain

$$\Delta G_0 = -RT \cdot \ln P_c = -RT(\ln 10)^{-1} \log P_c \quad (47)$$

Partition coefficients are sometimes defined as a ratio of molar fractions (P_x) instead of a ratio of concentrations (P_c). These two partition coefficients are related by⁸

$$P_x = \frac{x''}{x'} = \frac{c'' \cdot V''_{\text{molar}}}{c' \cdot V'_{\text{molar}}} = P_c \cdot \frac{V''_{\text{molar}}}{V'_{\text{molar}}}, \quad (48)$$

where x' and x'' are the molar fractions of the partitioning compound and V'_{molar} and V''_{molar} the molar volumes of the media.

Generalization to a system with several solutes results in independent partition coefficients as long as the compounds do not interact with each other. This independence of partition coefficients has been used when measuring octanol-water partition coefficients of several chlorophenols simultaneously (Schellenberg et al., 1984).

4.1.2 The Octanol-Water System

a) Description of the Bulk Phases

When performing the experiments, octanol and water phases are no longer pure. Water was found to be highly soluble in octanol, whereas octanol has a small solubility in water. The equilibrium concentrations of water in octanol reported in literature are 1.7 M according to Miller et al. (1985) and 2.3 M according to

⁸ We used the approximation $x = \frac{n_A}{n_A + n_{\text{medium}}} \approx \frac{n_A}{n_{\text{medium}}}$ for diluted solutions, where n_A is the number of moles of the partitioning compound and n_{medium} the number of moles of the solvent.

Leo et al. (1971) In contrast, octanol solubility in water is low, about 4.5 mM (Leo et al., 1971).

The effect of octanol solubility in water can be neglected with regard to volume changes⁹. But the small volume of octanol in the aqueous phase may still alter the aqueous solubility of 2,4,6-TrCP. The solubilities of DDT and hexachlorobenzene, two hydrophobic compounds, were, for example, enhanced by 160 and 80%, respectively to pure water (Chiou et al., 1982). On the other hand, no significant variation in solubility as a result of dissolved octanol in water was found for several other hydrophobic compounds (Miller et al., 1985). The effect of water solubility in octanol cannot be neglected, a 1.7 M concentration corresponds to a change in molar volume¹⁰ from pure octanol = 157 ml/mole to 127 ml/mole for saturated octanol, or a mole ratio of water to octanol of 1/3.5. The volume changes due to equilibration of water and octanol phases cannot be neglected, though it was found that the saturation of water in the octanol phase gives no significant differences in solubility between octanol saturated water and pure water for several hydrophobic compounds (Miller et al, 1985). The degree of saturation has also been seen to depend on the ionic strength of a solution and, by the use of buffers, on the pH. This variance in saturation occurs only for differences in salt which are quite high. By choosing the right experimental set-up, they can normally be neglected (Westall et al, 1990).

The effect of saturated phases on the thermodynamics in our experiments is considered to be constant due to our experimental set-up. We treat the

⁹ 4.5 mM octanol concentration in water corresponds to 0.7 ml of octanol in 1l of octanol saturated water.

¹⁰ The calculation of molar volume for the mixed state was done by assuming no volume change on mixing.

saturated octanol and saturated water phases as phases of constant composition which are not affected by the partitioning.

b) Distribution of Ionized and Un-ionized Species Between the Two Phases

The derivation of the molar partition coefficient P_c , Eq. 46, was done under the assumption that only one species or non-interacting species partition between the two phases. The existence of both ionized and un-ionized, neutral species, of 2,4,6-TrCP in the octanol-water system causes a complication. The goal of our experiment was to determine the partitioning of 2,4,6-TrCP as a function of pH and the individual partition coefficients for ionized (A^-) and neutral species (HA). If we assume that ionized and un-ionized species are only coupled by the pH and behave apart of that as independent solutes, the ideal partitioning can be applied to both of them.

The individual partition coefficients are not directly measurable but can be related to a measurable quantity, the total distribution coefficient of 2,4,6-TrCP between octanol and water. The total distribution coefficient, D , is given by

$$D = \frac{[HA]_{oc} + [A^-]_{oc}}{[HA]_{aq} + [A^-]_{aq}}, \quad (49)$$

where $[HA]_{oc}$ and $[A^-]_{oc}$ are the concentrations of neutral and ionized 2,4,6-TrCP in octanol, and $[HA]_{aq}$ and $[A^-]_{aq}$ are those in water. The individual partition coefficients are defined according to

$$g_{HA} = \frac{[HA]_{oc}}{[HA]_{aq}}, \quad (50)$$

$$g_A = \frac{[A^-]_{oc}}{[A^-]_{aq}}, \quad (51)$$

where g_{HA} is the partition coefficient of the neutral species and g_A the partition coefficient of the ionized species. $[A^-]_{aq}$ and $[HA]_{aq}$ are related to each other through the definition of pKa and pH. The pKa in water is defined as¹¹

$$pKa = -\log \frac{[H_3O^+][A^-]_{aq}}{[HA]_{aq}} \quad (52)$$

which yields together with $pH = -\log[H_3O^+]$

$$[A^-]_{aq} = [HA]_{aq} 10^{pH-pKa} \quad (53)$$

Substituting this equation and the definitions of g_A and g_{HA} into Eq. 49 results in

$$D = \frac{g_{HA} + g_A \cdot 10^{pH-pKa}}{1 + 10^{pH-pKa}}. \quad (54)$$

This equation relates the measurable quantities D, pH and pKa to the unknown g_A and g_{HA} . The individual partition coefficients g_A and g_{HA} can be obtained

¹¹ Activity coefficients are set equal to unity.

from the fit of Eq. 54 to the measured pH dependence of the total distribution coefficient D . For $\text{pH} \ll \text{pKa}$ the distribution coefficient D converges to g_{HA} and to g_{A} for $\text{pH} \gg \text{pKa}$. Furthermore, measurements of the total distribution coefficient D at the limiting pH values offer, an independent way to determine g_{A} and g_{HA} , in addition to nonlinear fit, Eq. 54.

4.1.3 The Water-Membrane System

The partitioning between water and membrane is often described with a linear partition coefficient, β_{X} , which relates the surface density of the compound X in the membrane, $(\text{X})_{\text{m}}$, to its bulk aqueous concentration, $[\text{X}]_{\text{aq}}$:

$$\beta_{\text{X}} = (\text{X})_{\text{m}} / [\text{X}]_{\text{aq}} \quad (55)$$

This linear partition coefficient is a useful tool to describe adsorption measurements to membranes.¹² To compare the water-membrane system with the octanol-water system a bulk partition coefficient for the membrane-water system is needed.

A bulk partition coefficient, γ_{X} for the membrane-water system can be defined as

$$\gamma_{\text{X}} = \langle [\text{X}]_{\text{m}} \rangle / [\text{X}]_{\text{aq}}, \quad (56)$$

¹² Adsorption of ionized chlorophenols was determined from changes of electrophoretic mobility of phosphatidylcholine liposomes (Blochel, 1992)

where $\langle [X]_m \rangle$ is the average membrane concentration of X

$$\langle [X]_m \rangle = \frac{\int_0^t [X(z)]_m \cdot dz}{t}, \quad (57)$$

where $[X(z)]_m$ denotes the local concentration, inside the membrane, at a distance z from the surface and t denotes the membrane thickness.

Using the symmetry of a bilayer and the definition of the linear partition coefficient, the bulk partition coefficient can also be expressed as

$$\gamma_X = 2\beta_X/t. \quad (58)$$

The bulk partition coefficient γ_X is related to the free energy of transfer of the species X. Therefore, $\log(\gamma_X)$ is proportional to the free energy of transfer from the bulk aqueous phase into the membrane.

4.2 Spectrophotometric Measurements

Molecules which can be excited to higher energy levels with visible or ultraviolet light can be detected by means of ultraviolet/visible (UV/VIS) spectrophotometry. Chlorophenols, as other conjugated organic compounds, absorb electromagnetic energy on their transition to higher energy levels. The quantum of electromagnetic energy is:

$$E = h\nu = \frac{hc}{\lambda} \quad (59)$$

On return to the ground state, the quantized radiant energy needed for the excitation of the molecules is set free and transformed into other energy forms, mostly thermal energy. Because of this transformation the different energy states of molecules can be observed by means of a spectrophotometer.

Transitions between different energy levels in the range of ultraviolet and visible light correspond basically to changes in the electronic energy though the total energy of a molecule depends on the sum of electronic, vibrational and rotational energies. The magnitude of vibrational and even rotational energies is much smaller than the electronic energy and causes only a splitting in the electronic energy levels, as shown in Figure 13, for a diatomic molecule. This splitting cannot be observed by conventional UV/VIS spectrophotometry because the resolution of spectrophotometers is limited. Instead of discrete absorption lines one observes absorption bands. The characteristic electron transition energies and their transition probabilities result in a characteristic spectrum which can be used for qualitative and quantitative analysis.

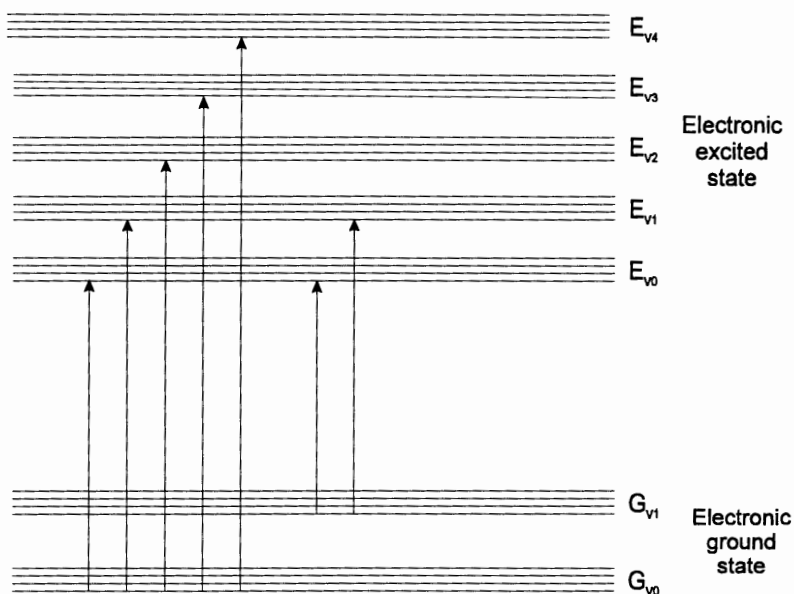


Figure 13. Energy level diagram of a diatomic molecule. The electronic ground state is labeled with G_{v_i} , the electronic excited state with E_{v_i} , where $i = 0, 1, 2, 3$ and 4 . The vibrational states designated v_i , split into different levels due to the rotational energies as indicated by the individual lines within each vibrational band (Silverstein, 1991).

4.2.1 Lambert-Beer's-Law

In our experiments we used quantitative analysis of spectra to determine the concentration of solutes in octanol and water phases. The concentration of a solute can be obtained from Lambert-Beer's law,

$$I(x) = I(0)e^{-A} \quad (60)$$

where $I(0)$ is the intensity of the radiant energy striking the sample, $I(x)$ the intensity of the radiation emerging from the sample after passing through a path length x and A is the absorbance. The absorbance depends, in turn, on the extinction coefficient of the solute, ϵ , its concentration, c , and the path length, x .

$$A = \epsilon cx, \quad (61)$$

The probability of the interaction between the radiant energy and the molecules increases with increasing concentration and causes an increase in the light absorption. The extinction coefficient is a characteristic constant of the solute-solvent system. Lambert-Beer's law is applicable to relatively transparent solvents and for solute concentrations at which solute-solute interactions are negligible. The absorbance of the whole sample can be expressed as

$$A = A_{solv} + A_{solute} \quad (62)$$

$$A_{solv} = \epsilon_{solv} c_{solv} x \quad \text{and} \quad A_{solute} = \epsilon_{solute} c_{solute} x$$

The total absorbance is the sum of solvent and solute absorbances. Absolute absorbance of the solute, A_{solute} , can be obtained by subtracting the absorbance of the pure solvent, A_{solv} , from the total absorbance.

4.2.2 Solvent Effects

The solvent, does in fact, have a great influence on the UV/VIS spectrum of the solute due to solvent-solute interactions. The acidity of the solvent determines the degree of dissociation of ionizable solutes, such as chlorophenols, and changes, in this way, their electronic configuration. This is reflected by changes of the UV/VIS absorption spectra.

Another type of solvent effect is related to the polarity of the solvent. Shifts in absorption spectra are observed as a function of the polarity of the solvent. An increase in polarity of the solvent will cause a bathochromic shift (shift to longer wavelengths) for $\pi \rightarrow \pi^*$ absorption bands, and a hypsochromic shift (shift to shorter wavelengths) for $n \rightarrow \pi^*$ absorption bands.

Furthermore, formation of micelles in the solvent gives rise to scattering effects which also alter the spectrum of the solute measured by a spectrophotometer. The intensity of scattering depends on the size of the micelles. The scattering is prominent at wavelengths of the same order as the size of the micelles and the intensity of light scattering increases with decreasing wavelength.

5 Materials and Methods

5.1 Chemicals

2,4,6-Trichlorophenol (98%) and 1-octanol (99+%), HPLC grade, were obtained from Aldrich Chemical Company (Milwaukee, WIS). Boric acid and potassium phosphate dibasic were bought from Mallinckrodt (St. Louis, MO), potassium chloride from EM Science (Cherry Hill, NJ) and potassium citrate from MCB Manufacturing Chemists (Cincinnati, Ohio). They were all used without further purification. The aqueous solutions were prepared with deionized water.

5.2 Instruments and their Specifications

The weighing of chemicals for preparation of all stock solutions was done using a balance from Mettler Instrument, Type H16 (Hightstown, NJ). The estimated accuracy of this model is ± 0.1 mg.

All pH measurements were done using a micro computer based pH meter, model 6072, from Jenco Electronics (Taipei, Taiwan). This pH meter has a ± 0.01 pH accuracy.

The spectrophotometer used for all concentration measurements was Model DU-7HS from Beckman Instruments (Irvine, CA). The following specifications of this spectrophotometer are important for the determination of

the accuracy of our measurements. The specifications are as follows: ± 0.5 nm wavelength accuracy, $\pm 0.5\%$ photometric accuracy, baseline drift < 0.003 Abs/hr and ± 0.001 Abs baseline flatness.

Throughout the study we used well matched pairs¹³ of quartz cuvettes as sample cells. For the buffer phase we used 1 mm¹⁴ and 50 mm cuvettes from Spectrocell Corporation (Oreland, PA) and 10 mm cuvettes from Pyrocell Manufacturing Co., Inc (Westwood, NJ). Spectra in the octanol phase were obtained with 10 mm cuvettes from Spectrocell Corporation (Oreland, PA).

The analysis of all data and the graphics were done with Axum V.4 for Windows.

5.3 Preparation of Octanol and Aqueous Phases

The aqueous phase, also called buffer phase, consists of a phosphoric acid/potassium citrate/boric acid (2mM/2mM/0.5mM) buffer with a salt concentration of 0.03M KCl. The solution was prepared from a 100 times concentrated buffer solution and a 2M KCl stock solution. The addition of KCl was needed to achieve the same experimental conditions as in the membrane adsorption measurements (Blochel, 1992) and to obtain, for all experiments, the same potassium concentration¹⁵.

¹³ Well matched pairs means in this context that the absorbance difference of such a pair should be less than 0.005.

¹⁴ The path lengths of the 1 mm cuvettes were actually determined to be $L = 1.12 + 0.01$ mm and $L = 1.11 + 0.02$ mm.

¹⁵ The partitioning of the ionized species of 2,4,6-Trichlorophenol is strongly dependent on the K^+ -concentration in the aqueous phase (Westall, 1985).

Octanol and buffer phases were preequilibrated before all experiments. This was necessary since octanol and water are partially miscible as described in 4.1.2 a. The miscibility affects the volume and the spectroscopic properties of the octanol and buffer phases. These two phases were mutually equilibrated before all experiments and an octanol/water ratio of 1:5 was used. Octanol and buffer phases were mixed for one hour with a Wrist-Action shaker model BB from Burrell Corp. (Pittsburgh, PA) in 250 ml polypropylene centrifuge bottles, and afterwards centrifuged at 1500 g with a IEC DPR-600 centrifuge.

The separation of the two phases was performed by removing the octanol-phase from the top of the bottles with a syringe. The buffer phase was sucked out with a 100 ml pipette. Both the octanol and the buffer phases were collected from each batch¹⁶ and measured spectrophotometrically using the corresponding unsaturated phases as background. Spectrophotometric measurements were necessary to examine the effect of phase saturation and to verify that the method of equilibration was reproducible.

It was found that the buffer phase is only slightly affected by saturation with octanol, see Figure 14. The difference in absorbance between the saturated and the unsaturated phases was always smaller than 0.01. The octanol phase, see Figure 15, always shows two peaks, one at about 225 nm with absorbance varying between 0.1 and 0.6 and the other at about 276 nm with absorbance varying between 0.04 and 0.09. The reason for these peaks is unknown, the absorbance at these wavelength occurs probably as a result of the formation of water micelles in the octanol phase. The variation of the absorbance between samples can be explained as a function of the variation in the concentration of water micelles in octanol from batch to batch.

¹⁶ Each batch consists of about 4-6 centrifuge bottles.

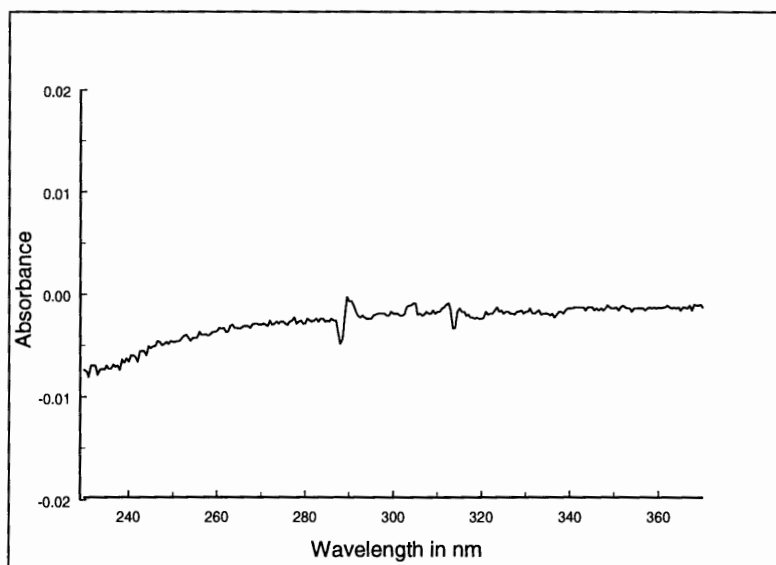


Figure 14. Typical spectrum of the saturated buffer phase, measured against pure buffer.

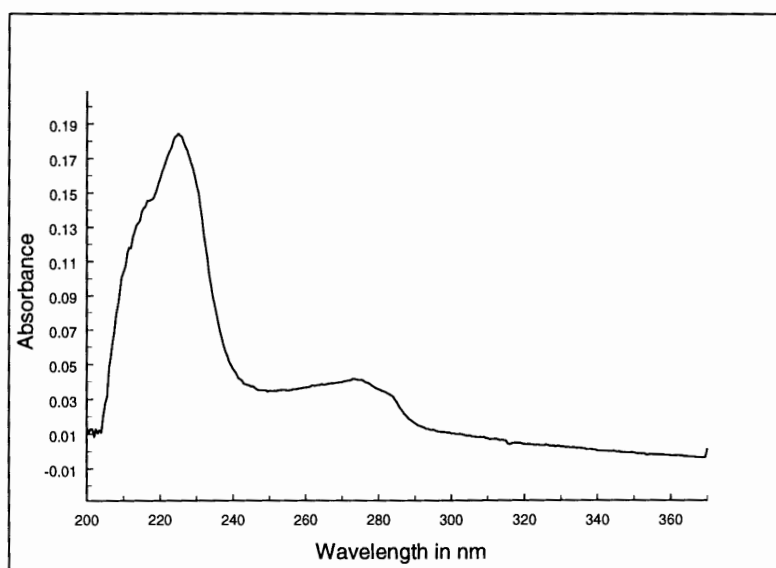


Figure 15. Typical spectrum of the saturated octanol phase, measured against pure octanol.

5.4 Extinction Coefficients

The distribution of 2,4,6-TrCP between the octanol phase and the buffer phase was determined by spectroscopic determination of the concentration of 2,4,6-TrCP in the octanol and the buffer phases. Therefore, as a first step, the extinction coefficients of 2,4,6-TrCP in octanol-saturated buffer and water-saturated octanol were determined.

The absorbance of 2,4,6-TrCP is pH dependent due to its ionization. The neutral form has an absorbance peak at 293 nm and in its ionized form at 311.5 nm. For all concentration determinations in the aqueous phase, 2,4,6-TrCP was converted into its ionized form by adjusting the pH to about 10-11.¹⁷ Due to this simplification of the experimental protocol it was necessary to determine the extinction coefficients only for the ionized species.

The applicability of Lambert-Beer's law was tested for sample concentrations between 40 and 200 μM . Those were prepared from four different stock solutions (1-3 mM). The stock solutions were prepared with unsaturated buffer because at such high 2,4,6-TrCP concentrations 2,4,6-TrCP tends to aggregate with octanol present in the aqueous phase. Saturated buffer was then used for the dilution of the stock solutions to the different sample concentrations. The sample solutions were titrated with KOH to pH \sim 10-11 and the absorbance determined in 1 cm cuvettes.

The extinction coefficient in saturated octanol was measured for sample concentrations between 0.1 and 0.6 mM, prepared from stock solutions 5-6 mM.

¹⁷ The pKa of 2,4,6-TrCP is 6.1 (Schellenberg, 1984), a titration to pH \sim 10-11 corresponds therefore to more than 99.9% ionization of 2,4,6-TrCP.

5.5 Partitioning

The partitioning experiment was performed with two different sets of preequilibrated phases. The first set consisted of three different batches. Saturated octanol and aqueous phases from these three batches were respectively collected and used for as follows:

First, 100 ml of a 20 mM 2,4,6-TrCP of water-saturated octanol solution was prepared. Then for each partitioning experiment we used 5ml of this 2,4,6-TrCP saturated octanol stock solution to which we added 25 ml of pH adjusted saturated buffer. The pH of the saturated buffer phase was set to values between 4.91 and 12.77 by the addition of HCl or KOH. The sample containing 25 ml of the pH adjusted buffer and the 5 ml of the 20 mM 2,4,6-TrCP saturated octanol were mixed in 50 ml glass tubes, shaken for one hour (with the same shaker used for the phase saturation) and were afterwards centrifuged at 1500 g for one hour in a Safeguard centrifuge from Clay-Adams Inc. (New York, NY). Since the samples warm up during the centrifugation step it was necessary to postpone the analysis an hour after centrifugation that the samples are re-equilibrated at the test temperature.

The sample analysis protocol included pH and 2,4,6-TrCP concentration measurements of the buffer phase. The pH of the buffer phase had to be measured after the partitioning since 2,4,6-TrCP is a weak acid and changes the pH. The final pH ranged from 4.98 to 12.72. The concentration of 2,4,6-TrCP in the buffer was determined after the pH -measurement and after titrating the sample to pH ~ 10-11. The three different cuvette pairs (1, 10, 50 mm) were used depending on the concentration of 2,4,6-TrCP.

A second set of partitioning experiments were performed with only one batch of saturated phases. In this cases 50 ml of 64 mM 2,4,6-TrCP water-saturated octanol solution was used and the final pH varied between 3.49 and 7.72. Apart from that the preparation and measurement methods were the same as in the first run.

For both runs the experimental protocol was designed to minimize the errors involved in all measurements: (a) The number of sets of preequilibrated phases used to perform the experiment was reduced to two, (b) the ratio of octanol to buffer phase was the same, 5:1, for both the partitioning experiment as well as the phase presaturation.¹⁸ (c) 2,4,6-TrCP stock solutions in octanol, rather than in buffer, were used because of the higher solubility of 2,4,6-TrCP in octanol which made it possible to weigh manageable amounts of 2,4,6-TrCP (about 390 and 630 mg) and thus to obtain well defined stock solution. The use of stock solutions has the additional advantage of maintaining the total concentration of 2,4,6-TrCP constant which makes it then possible to obtain a meaningful plot of 2,4,6-TrCP concentrations in the two phases versus pH, in addition to the pH dependence of the total distribution coefficient.

¹⁸ A possible change in the degree of saturation due to different saturation methods is therefore nearly excluded.

6 Results

6.1 Extinction Coefficients

6.1.1 Results

The extinction coefficients of 2,4,6-Trichlorophenol in buffer (ϵ_{buf}) and octanol (ϵ_{oc}) have been measured for several concentrations using 1 cm cuvettes. Characteristic absorbance spectra for 2,4,6-TrCP are shown in Figure 16 for octanol and in Figure 17 for buffer. Table 1 lists the values for the extinction coefficient obtained for the buffer and Table 2 for the octanol. The average extinction coefficient in the buffer phase was calculated, including the measured values in pure buffer. No measurable differences between ϵ_{buf} in the pure and the saturated buffer could be detected. The average peak extinction coefficients are:

4800 ± 150 1/Mcm (at $\lambda = 311.5$ nm) for ionized 2,4,6-TrCP in the octanol saturated buffer, and

2900 ± 70 1/Mcm (at $\lambda = 297.5$ nm) for un-ionized 2,4,6-TrCP in the water saturated octanol.

6.1.2 Error Calculations

The standard deviation or the statistical error of both extinction coefficients is about 3% and can be explained by the errors involved in both the sample preparation and in the measurements of the absorbance. Error calculation was done to gain insight into the different origins of errors. The maximum error of the extinction coefficients was calculated using the following general relation for the absolute maximum error:

$$\Delta F = \pm \left(\left| \frac{\partial F}{\partial x} \Delta x \right| + \left| \frac{\partial F}{\partial y} \Delta y \right| + \dots \right) \quad (63)$$

ΔF stands for the maximum absolute error of a measured quantity F ; Δx , Δy ,... are the estimated errors of the measured values.

The error of weighing was estimated to be ± 0.1 mg and the error of all volumetric measurements to be 1%. Applying Eq. 63, the maximum error resulting from weighing and the different volumetric measurements varies between 3.4% and 4.3%. The maximum error resulting from absorbance measurements (estimated error ± 0.005) varies between 0.4 % and 2.4 %. Therefore, the total errors range from 3.7% to 6.3% and are consistent with the the magnitude of the standard deviations of extinction coefficients.

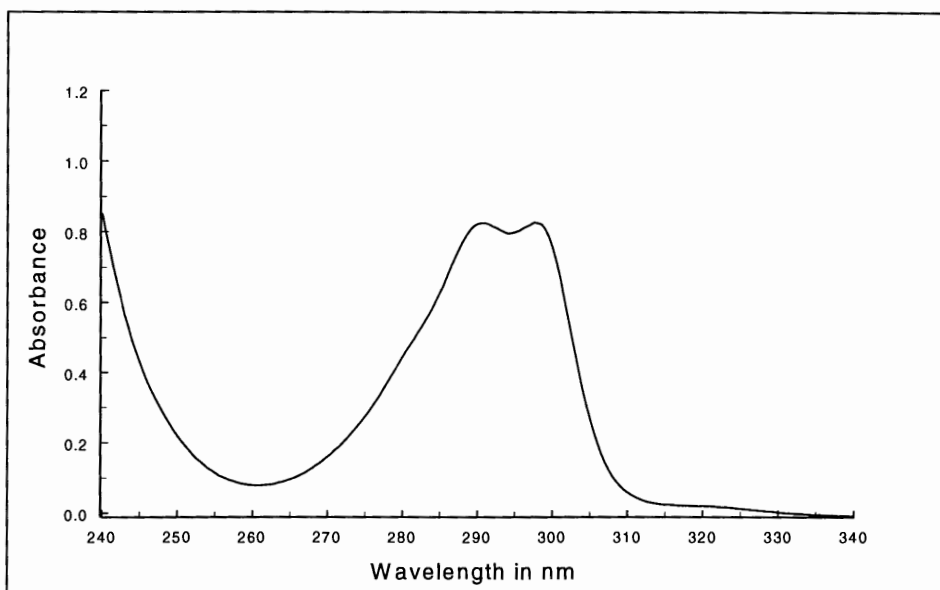


Figure 16. Spectrum of un-ionized 2,4,6-TrCP (285 μM) in water-saturated octanol.

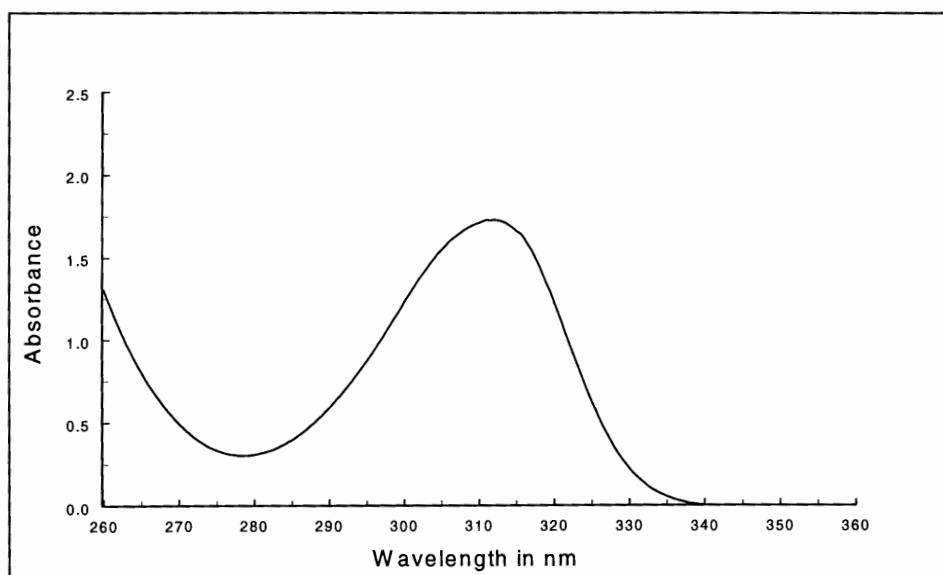


Figure 17. Spectrum of ionized 2,4,6-TrCP (36 μM) in octanol-saturated buffer.

solvent	stock concentration [mM]	sample concentration [μ M]	pH	absorbance at $\lambda = 311.5$ nm	extinction coefficient [1/M·cm]
B-3	2.73	109	~10	0.524	4800
B-3	2.73	109	~10	0.534	4900
B-3*	1.08	43	10.44	0.213	5000
B-3*	1.08	86	10.14	0.418	4900
B-3*	1.22	120	10.28	0.599	5000
B-3*	1.22	168	10.42	0.842	5000
B-3*	1.22	72	10.44	0.356	4900
B-3*	1.09	54	10.30	0.250	4700
B-3*	1.09	107	10.20	0.494	4600
B-3*	1.09	213	10.72	0.989	4600

average extinction coefficient = 4800 ± 150 ($\lambda = 311.5$ nm)

Table 1. Extinction coefficients of 2,4,6-Trichlorophenol in buffer; B-3 designates unsaturated aqueous phase, B-3* the octanol-saturated aqueous phase.

solvent	stock concentration [mM]	sample concentration [μ M]	absorbance at $\lambda = 297.5$ nm	extinction coefficient [1/M·cm]
Oct*	5.46	328	.961	2930
Oct*	5.46	437	1.242	2840
Oct*	5.46	546	1.572	2880
Oct*	5.46	219	.616	2820
Oct*	5.46	328	.994	3030
Oct*	5.68	341	.997	2920
Oct*	5.68	114	.332	2920

average extinction coefficient = 2900 ± 70 ($\lambda = 297.5$ nm)

Table 2. Extinction coefficients of 2,4,6-Trichlorophenol in water-saturated octanol.

6.2 Partitioning

6.2.1 Results

The octanol-water partition experiment was performed with two different initial concentrations¹⁹ of 2,4,6-TrCP in saturated octanol to obtain the pH-dependence of the distribution for the pH from 3.5 to 12.7. Two initial concentrations of 2,4,6-TrCP in saturated octanol were necessary in order to obtain data at $\text{pH} \ll \text{pK}_a$ and $\text{pH} \gg \text{pK}_a$.

In most cases the distribution of 2,4,6-TrCP was based on measurements of 2,4,6-TrCP in the buffer phase. In the buffer phase the 2,4,6-TrCP concentration changes, as a function of pH, by several orders of magnitude whereas the concentration in the octanol phase remains about the same. The 2,4,6-TrCP concentrations in the octanol phase were calculated using the mass conservation of 2,4,6-TrCP. The mass balance of 2,4,6-TrCP was verified experimentally several times by measuring the concentration of 2,4,6-TrCP in the octanol phase. The error in mass balance was random and varied between 1.5% and 6.9%. Those errors are within the limit of the measurement errors²⁰, errors which were about 10%. Therefore, within the limits of the concentration measurement the mass was conserved.

The experimentally measured buffer and octanol concentrations of 2,4,6-TrCP as a function of pH are shown in Table 4 and Table 5. These data were

¹⁹ The initial concentration is the 2,4,6-TrCP-concentration in the water-saturated octanol injected into the octanol phase.

²⁰ The measurement errors were calculated using Eq. 63.

used to obtain the total distribution coefficient according to Eq. 49. The octanol-water partition coefficients of the ionized, g_A , and the un-ionized species, g_{HA} , were obtained by fitting the pH dependence of $\log D$. A logarithmic fit of D was used since the relative error, and not the total error, was of physical interest.

It follows from the theory of the ideal partitioning (4.1.1) that the logarithm of partition coefficient is proportional to the free energy of transfer according to Eq. 47. Therefore, the fit of $\log D$ rather than that of D itself has greater physical meaning. In the limits of very low pH, $D \approx g_{HA}$ and in the limits of very high pH, $D \approx g_A$.

The best fit was obtained for the following octanol-water partition coefficients of individual species:

$$g_A = 1.42 \pm 0.16$$

$$g_{HA} = 4500 \pm 210$$

or expressed in terms of the decadic logarithm:

$$\log(g_A) = 0.15 \pm 0.05$$

$$\log(g_{HA}) = 3.65 \pm 0.02$$

The pH dependence of the measured total distribution coefficient D of 2,4,6-TrCP is given in Table 3. The experimental results as well as the theoretical predictions of the partition model for the best parameters are shown in Figure 18. Similar data for the concentrations in octanol and buffer phases are

presented in Table 4 and Table 5 and Figure 19 and 20. The gray lines illustrate the standard deviation of the predicted values.

The plot of the total distribution coefficient for the best parameters was done using Eq. 54. The plot of the concentrations in the octanol and buffer phases was based on the mass balance and the definition of the total distribution coefficient, Eq. 49. The mass balance is given by

$$\left([\text{HA}]_{\text{aq}} + [\text{A}^-]_{\text{aq}}\right) \cdot \text{vol}_{\text{aq}} + \left([\text{HA}]_{\text{oc}} + [\text{A}^-]_{\text{oc}}\right) \cdot \text{vol}_{\text{oc}} = [\text{HA}]_{\text{input}} \cdot \text{vol}_{\text{oc}},$$

where $([\text{HA}]_{\text{aq}} + [\text{A}^-]_{\text{aq}})$ and $([\text{HA}]_{\text{oc}} + [\text{A}^-]_{\text{oc}})$ are the equilibrium concentrations of 2,4,6-TrCP in the buffer and octanol phase, and $[\text{HA}]_{\text{input}}$ the initial concentration of 2,4,6-TrCP in the octanol phase. The quantities vol_{aq} and vol_{oc} designate the buffer and octanol volume. The mass balance together with Eq. 49 results in the following expression for the total concentration in the buffer phase

$$\left([\text{HA}]_{\text{aq}} + [\text{A}^-]_{\text{aq}}\right) = \frac{[\text{HA}]_{\text{input}}}{\text{vol}_{\text{aq}}/\text{vol}_{\text{oc}} + D}$$

The total concentration in the octanol phase predicted from the partition model

$$\left([\text{HA}]_{\text{oc}} + [\text{A}^-]_{\text{oc}}\right) = \frac{D \cdot [\text{HA}]_{\text{input}}}{\text{vol}_{\text{aq}}/\text{vol}_{\text{oc}} + D}$$

The value of the partition coefficient of the un-ionized species of 2,4,6-TrCP, obtained in this study, $\log(g_{\text{HA}}) = 3.65 \pm 0.02$, is in good agreement with

literature values that range from 3.38 to 3.72 (Schellenberg et al., 1984; Callahan et al., 1979; Xie et al., 1984 and Hansch, 1971). The value of the partition coefficient of the ionized species of 2,4,6-TrCP is several orders smaller compared to that of the un-ionized species. There are no literature values of the octanol-water partition coefficients for the ionized species of 2,4,6-TrCP.

6.2.2 Error Calculations

The confidence limits of the partition parameters associated with their standard deviation are shown as grey lines in Figure 18, 19, 20. The maximum experimental errors calculated from Eq. 63 are shown as error bars. The total distribution coefficients are listed in Table 3. The concentration data are summarized in Table 4 and Table 5. The following errors were taken into account in the error calculations:

- standard deviations of the measured extinction coefficients
- errors in the saturated buffer and octanol volumes, these were estimated to be 1%
- error in absorbance measurement, estimated as ± 0.005 absorbance units
- error in the path length of the cuvettes, estimated as 2%
- error in weighing (estimated as ± 0.1 mg)

In general, the errors of all error sources increase with the decreasing value of $\log D$. This can be clearly seen in the data in Table 3. The logarithmic fit due to these errors is better at low pH values rather than at high pH values.

final pH	$D = \frac{[HA]_{oc} + [A^-]_{oc}}{[HA]_{aq} + [A^-]_{aq}}$	ΔD [%]	log D	$\Delta \log D$ [%]
3.49	4.24e+3	7.02	3.63	1.93
4.74	4.43e+3	7.05	3.65	1.93
4.98	3.19e+3	9.11	3.50	2.60
5.60	2.30e+3	6.56	3.36	1.95
6.10	2.92e+3	8.81	3.47	2.54
6.54	1.08e+3	6.68	3.03	2.20
6.77	8.71e+2	6.99	2.94	2.38
7.13	3.74e+2	6.02	2.57	2.34
7.57	1.80e+2	8.49	2.26	3.76
7.72	1.05e+2	7.54	2.02	3.73
7.76	1.06e+2	6.72	2.03	3.31
7.88	7.14e+1	6.46	1.85	3.49
8.15	4.27e+1	8.94	1.63	5.48
8.66	1.68e+1	9.05	1.23	7.83
9.82	2.65e+0	20.7	0.422	48.8
11.68	1.27e+0	36.5	0.102	355
12.72	1.43e+0	32.9	0.156	210

Table 3. Experimental data and calculated error for the pH dependence of the total distribution coefficient of 2,4,6-Trichlorophenol between octanol and water.

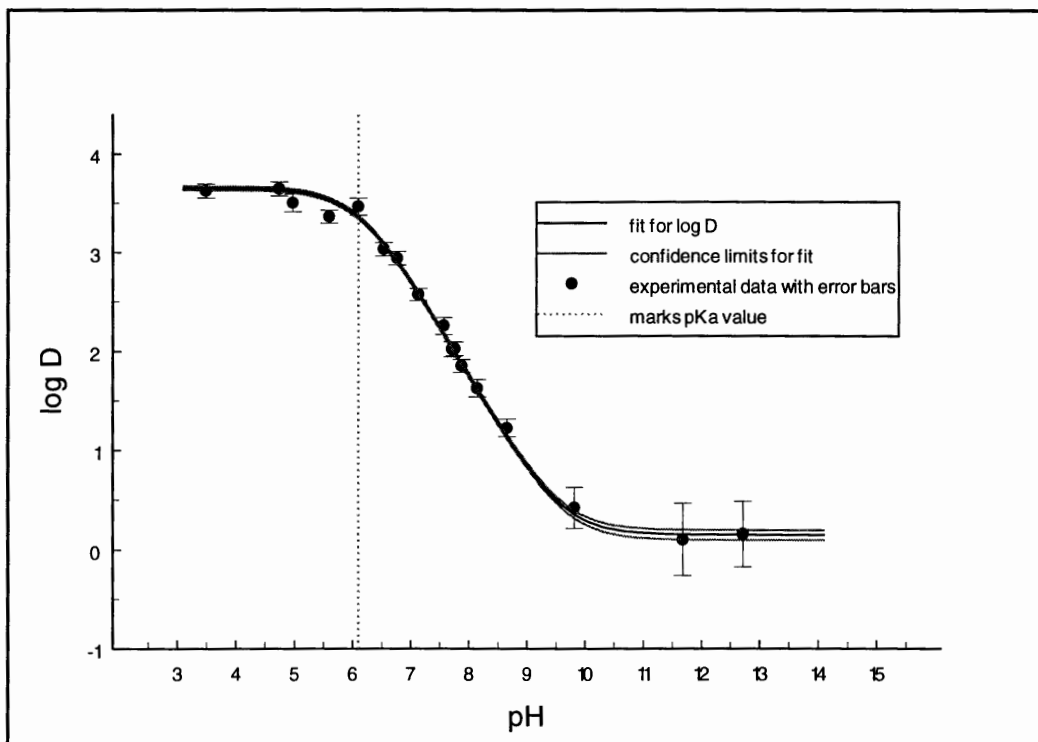


Figure 18. The pH dependence of the total distribution coefficient D of 2,4,6-Trichlorophenol between octanol and water.

final pH	$[HA]_{aq} + [A^-]_{aq}$ [mM]	$\Delta([HA]_{aq} + [A^-]_{aq})$ [%]	$[HA]_{oc} + [A^-]_{oc}$ [mM] calculated with mass balance
4.98	6.16e-3	8.97	1.97e+1
6.10	6.74e-3	8.66	1.97e+1
6.54	1.82e-2	6.51	1.96e+1
7.13	5.21e-2	5.79	1.95e+1
7.76	1.77e-1	6.20	1.88e+1
7.88	2.58e-1	5.78	1.84e+1
8.15	4.13e-1	7.67	1.77e+1
8.66	9.02e-1	6.40	1.52e+1
9.82	2.58e-0	5.71	6.83e+0
11.68	3.15e-0	5.65	3.99e+0
12.72	3.02e-0	5.65	4.40e+0

Table 4. Experimental results. Total aqueous and octanol concentrations of 2,4,6-TrCP obtained for the 20 mM initial concentration of 2,4,6-TrCP in octanol, $\Delta([HA]_{aq} + [A^-]_{aq})$ designates the calculated maximum error.

final pH	$[HA]_{aq} + [A^-]_{aq}$ in mM	$\Delta([HA]_{aq} + [A^-]_{aq})$ in %	$[HA]_{oc} + [A^-]_{oc}$ in mM, calculated with mass balance	$[HA]_{oc} + [A^-]_{oc}$ in mM, experimental data
3.49	1.51e-2	6.89	6.40e+1	6.85e+1
4.74	1.44e-2	6.92	6.40e+1	5.87e+1
5.60	2.77e-2	6.42	6.39e+1	6.40e+1
6.77	7.31e-2	6.82	6.37e+1	5.68e+1
7.57	3.46e-1	8.09	6.23e+1	5.74e+1
7.72	5.80e-1	6.99	6.12e+1	5.97e+1

Table 5. Experimental results. Total aqueous and octanol concentrations of 2,4,6-TrCP obtained for the 64 mM initial concentration of 2,4,6-TrCP in octanol, $\Delta([HA]_{aq} + [A^-]_{aq})$ designates the calculated maximum error.

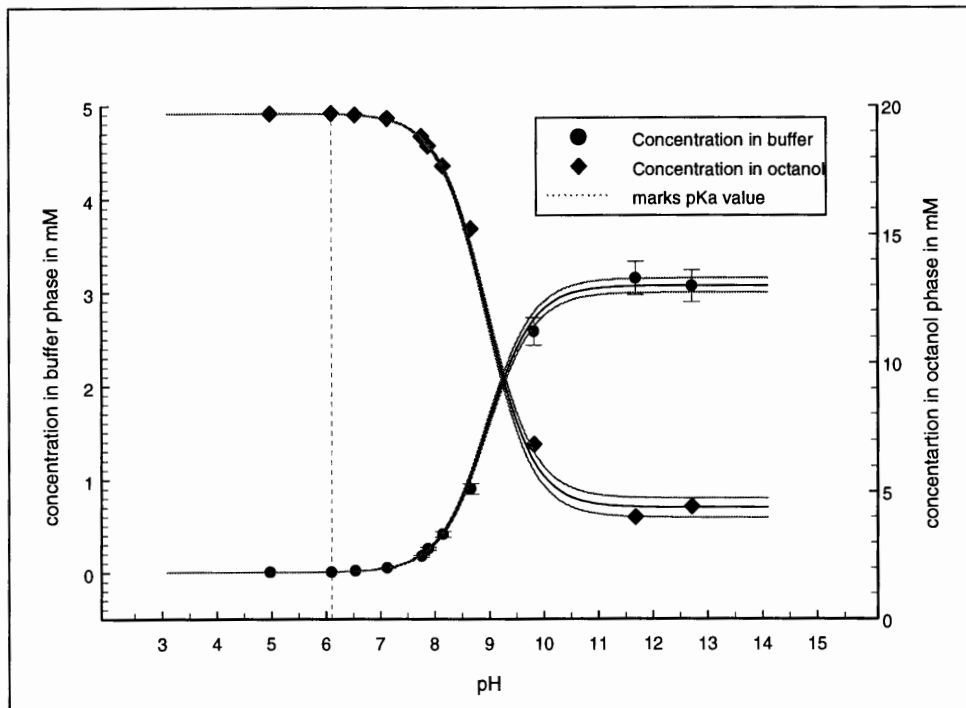


Figure 19. pH dependence of 2,4,6-TrCP concentrations in buffer (left axis) and octanol (right axis) obtained with 20 mM initial octanol concentration of 2,4,6-TrCP. The solid curves illustrate prediction of the partition model for the best fit parameters. The error bars illustrate maximum experimental error.

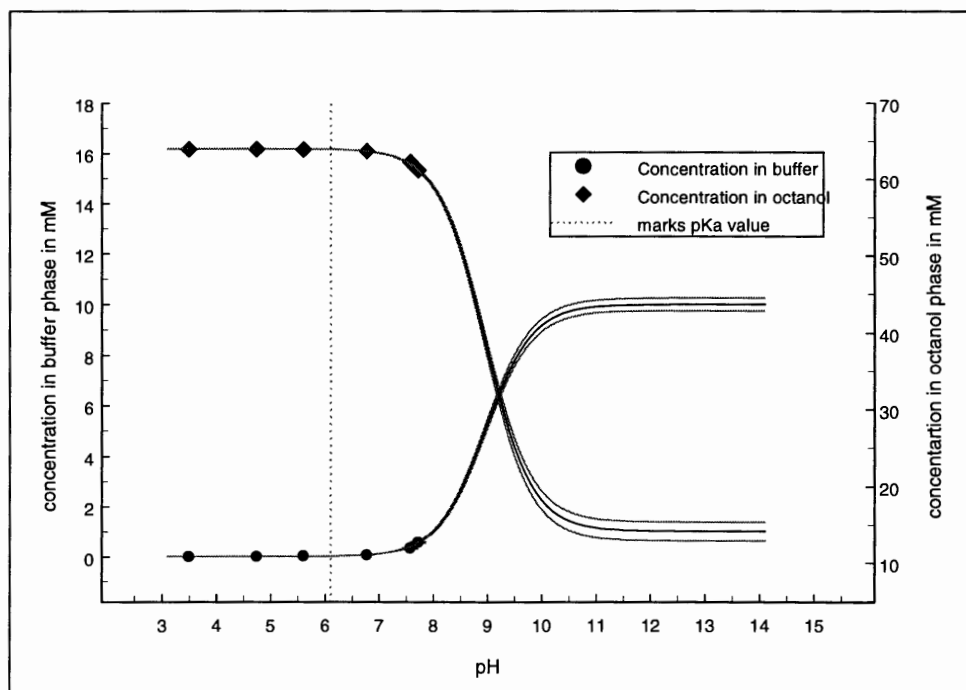


Figure 20. pH dependence of 2,4,6-TrCP concentrations in buffer (left axis) and octanol (right axis) obtained with 64 mM initial octanol concentration of 2,4,6-TrCP. The solid curves illustrate prediction of the partition model for the best fit parameters. The error bars illustrate maximum experimental error.

7. Discussion

7.1 Comparison of the Octanol-Water System with the Membrane-Water System

The knowledge of the octanol-water partition coefficient of the ionized species of 2,4,6-TrCP, g_A , makes it possible to compare its value with that obtained for the lipid membrane water system. Blochel (1994) measured the linear partition coefficient, β_A , of ionized 2,4,6-TrCP for lipid membranes and obtained, $\beta_A = (6.55 \pm 0.33) \cdot 10^{-7}$ m. The linear partition coefficient β can be related to the octanol-water partition coefficient after transformation using Eq. 58, to obtain the bulk partition coefficient of ionized species for lipid membranes γ_A . Using a membrane thickness of $t = 3.8$ nm (McIntosh and Simon, 1986) one obtains then a bulk partition coefficient $\gamma_A = (3.45 \pm 0.17) \cdot 10^2$. The value of γ_A is about 240 times greater than that predicted by the octanol-water partition coefficient. Similar behavior was found for 2,3,4,5-Tetrachlorophenol which was studied by Schmidt (1995) using the same experimental methods and for pentachlorophenol (Smejtek and Wang, 1993). The partition coefficients of these three different chlorophenols are shown in Table 6.

molecular species	$\log \gamma_A^a$	$\log g_A$	$\frac{\log g_A}{\log \gamma_A}$	$\log g_{HA}$	$\frac{\log g_{HA}}{\log \gamma_A}$
2,4,6-TrCP	2.538 ± 0.022	0.15 ± 0.05	0.0591	3.65 ± 0.02	1.44
2,3,4,5-TeCP	3.475 ± 0.015	0.87 ± 0.10^b	0.250	4.52 ± 0.05^b	1.30
PCP	4.281 ± 0.02	1.48^c	0.346	5.08^d	1.19

a: Blochel (1994)

b: Schmidt (1995)

c: in 0.1 M KCl (Jafvert and Westall, 1990)

d: Xie (1984)

Table 6. Comparison of bulk partition coefficients of three different chlorophenols for lipid-membrane-water and octanol-water systems.

The following conclusions can be made:

- (a) The lipid-membrane-water partition coefficient γ_A is always several orders of magnitude greater than the octanol-water partition coefficient g_A . In view of this result the octanol-water partition coefficient is not a suitable tool for the prediction of distribution of the ionized form of the above chlorophenols between water and lipid membranes. It is to be expected that the octanol-water partition coefficient g_A seriously underestimate the concentration of ionized chlorophenols in biological membranes.
- (b) The partition coefficients for the membrane-water system as well as for the octanol-water system increase with the number of chlorine substituents on the benzene ring.

The differences of the partition coefficients of the membrane-water system and the octanol-water system can be based on the physical properties of the two model systems. The main difference is that octanol, as a bulk phase, requires maintainance of the electroneutrality and therefore co-partitioning of counterions which requires additional free energy. A description of the partition mechanism in the octanol-water system is given in Appendix B.

Appendix A

Derivations: The Gouy-Chapman Theory

Consider an infinite uniformly charged surface in contact with an infinite homogenous electrolyte. Ions in an electric field obey a Boltzmann distribution, Eq. 1, and cause a non-vanishing space charge density, Eq. 3. This in turn gives rise to an electric potential, Eq. 2. A combination of Eqs. 1, 2 and 3 results in the *Poisson-Boltzmann equation*

$$\frac{d^2\psi(z)}{dz^2} = -\frac{1}{\epsilon_r \epsilon_0} \sum_i z_i e N_i(\infty) \exp\left(-\frac{z_i e \psi(z)}{kT}\right) \quad (4)$$

The *Poisson-Boltzmann equation* is a nonlinear differential equation which has to be, in general, solved numerically. A first integration of Eq. 4 is analytically possible by use of the following transformation:

Multiplication of each side of Eq. 4 by $2 \frac{d\psi}{dz}$ and the use of the identity

$$2 \frac{d\psi}{dz} \frac{d^2\psi}{dz^2} = \frac{d}{dz} \left(\frac{d\psi}{dz} \right)^2 \text{ transforms Eq. 4 to}$$

$$\frac{d}{dz} \left(\frac{d\psi}{dz} \right)^2 = -2 \frac{d\psi}{dz} \frac{1}{\epsilon_r \epsilon_0} \sum_i z_i e N_i(\infty) \exp\left(-\frac{z_i e \psi(z)}{kT}\right). \quad (1a)$$

The *Poisson-Boltzmann equation* in this form Eq. 1a can then be easily integrated from z to infinity.

$$\left(\frac{d\psi}{dz}\right)^2 \Big|_z^\infty = -\frac{2kT}{\epsilon_r \epsilon_0} \sum_i N_i(\infty) \exp\left(-\frac{z_i e \psi(z)}{kT}\right) \Big|_z^\infty \quad (2a)$$

The boundary conditions are

$$\lim_{z \rightarrow \infty} \frac{d\psi}{dz} = 0 \quad \text{and} \quad \lim_{z \rightarrow \infty} \psi(z) = 0 \quad (3a)$$

This results in the nonlinear equation

$$\left(\frac{d\psi}{dz}\right)^2 = \frac{2kT}{\epsilon_r \epsilon_0} \sum_i N_i(\infty) \left[\exp\left(-\frac{z_i e \psi(z)}{kT}\right) - 1 \right]. \quad (4a)$$

The double layer consisting of the membrane surface charge and the space charge of opposite polarity in the aqueous phase have to be, as a whole, electrically neutral. Consequently, the charge on the surface of the membrane must be balanced by the charge in the solution; i.e.

$$\sigma_m = -\int_0^\infty \rho(z) dz, \quad (5a)$$

σ_m , denotes the surface charge density on the membrane surface. By substituting for $\rho(z)$, Eq. 2, into Eq. 5a we obtain

$$\sigma_m = \int_0^{\infty} \epsilon_r \epsilon_0 \frac{d^2 \psi(z)}{dz^2} dz \quad (6a)$$

which together with the boundary condition $\lim_{z \rightarrow \infty} \frac{d\psi}{dz} = 0$, can be integrated to yield

$$\sigma_m = -\epsilon_r \epsilon_0 \left. \frac{d\psi(z)}{dz} \right|_{z=0} \quad (7a)$$

The combination of Eqs. 4a and 7a results in the *Gouy-Chapman equation*,

$$\sigma_m = \pm \left[2 \epsilon_r \epsilon_0 kT \sum_i N_i(\infty) \left\{ \exp\left(-\frac{z_i e \psi(0)}{kT}\right) - 1 \right\} \right]^{\frac{1}{2}}, \quad (8a)$$

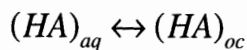
where $\psi(0)$ is the potential at the membrane surface.

Appendix B

The Partitioning in the Octanol-Water System: Multicomponent Partitioning

In the ideal partitioning theory, section 4.1.1, we assumed that the partitioning of a species depends on the free energy of transfer of this particular species and we neglected any interactions between different species. This idealization can not be applied to the partitioning of the ionized species. The partitioning of the ionized species is strongly coupled to the partitioning of counterions, in our experiment to potassium ions, K^+ , to satisfy the electroneutrality of the two phases. The partitioning of A^- has to be treated as a multicomponent chemical equilibrium problem rather than a single component equilibrium problem (Westall et al., 1985). The following reactions between the octanol and water bulk phases can qualitatively describe the partitioning of 2,4,6-TrCP, as suggested by Westall.

- (i) Solvation of the neutral organic compound in bulk octanol phase :



- (ii) Solvation of free ions or ion pairs in the bulk octanol phase :



where $(HA)_{aq}$, K_{aq}^+ and A_{aq}^- are the species in the aqueous phase, and $(HA)_{oc}$, K_{ocI}^+ , $(KA)_{ocII}$ and A_{ocI}^- are the species in the octanol phase. C_I and C_{II} are the dissociation coefficients of reaction I and II.

Reaction (i) describes the partitioning of the neutral species, which is an ideal partitioning process. The reactions suggested in (ii) show the dependence of A^- -partitioning on the ionic strength. In principal, the partitioning of A^- increases with the increasing ionic strength. The reactions (ii) are the most probable reactions to describe the sorption of the ionized form of 2,4,6-TrCP to the octanol phase. But sorption of A^- can also occur as adsorption¹ of A^- to the octanol, with a counterion in the electric double layer, or as a ligand exchange of the organic molecule with a surface hydroxyl group at the inorganic oxide surface. Those reactions which take place at the interface are thought to play a minor role in the sorption process as octanol and water are used as extended bulk phases.

Using the dissociation coefficients of the reactions in (ii),

$$C_I = \frac{[K^+]_{ocI} [A^-]_{ocI}}{[K^+]_{aq} [A^-]_{aq}} \Rightarrow \frac{[A^-]_{ocI}}{[A^-]_{aq}} = \frac{[K^+]_{aq}}{[K^+]_{ocI}} \cdot C_I$$

$$C_{II} = \frac{[(KA)]_{ocII}}{[K^+]_{aq} [A^-]_{aq}} \Rightarrow \frac{[A^-]_{ocII}}{[A^-]_{aq}} = [K^+]_{aq} \cdot C_{II}$$

¹ This is an adsorption mechanism like in the membrane-water system.

g_A can be expressed as

$$g_A = \frac{[A^-]_{oc}}{[A^-]_{aq}} = [K^+]_{aq} \cdot \left\{ \frac{C_I}{[K^+]_{ocI}} + C_{II} \right\}. \quad (1b)$$

Equation 1b shows the nonlinear dependence of g_A on the potassium concentration in the aqueous phase. The partition coefficient g_A increases with increasing potassium concentration. C_I and C_{II} are characteristic constants for the transport of K^+ and A^- , either as free ions (reaction I) or as ion pairs (reaction II), from the aqueous to the octanol phase. Experimental data from Schwarzenbach² (1985) predicted the existence of the free ions rather than ion pairs in the octanol phase. If we consider that this is also applicable to our system

$$[K^+]_{oc} = [A^-]_{oc} = \left([A^-]_{aq} [K^+]_{aq} C_I \right)^{1/2}$$

the expression for g_A can be simplified to

$$g_A = \frac{[A^-]_{oc}}{[A^-]_{aq}} = \left(\frac{[K^+]_{aq} \cdot C_I}{[A^-]_{aq}} \right)^{1/2} \quad (2b)$$

² Schwarzenbach measured the octanol-water distribution ratio of PCP and 2,3,4,5 TeCP at pH ~ 12 as a function of the ratio $[Na^+]/[A^-]$ and found linear relationship between $\log g_A$ and $[Na^+]/[A^-]$.

The important feature of either case, $C_{II} = 0$ or $C_{II} \neq 0$, is that the free energy of transfer of A^- -ions from the aqueous to the octanol phase depends on the energy needed not only to carry an A^- -ion but also K^+ -ion across the interface. $\text{Log}(g_A)$, which is proportional to the free energy of transfer, is therefore a function of the ionic strength in the aqueous phase. In view of this non-ideal behaviour the partitioning of A^- cannot be treated according to an ideal partitioning theory.

References

Aveyard, R. and D.A. Haydon. 1973. An introduction to the principles of surface chemistry. Cambridge University Press, Cambridge.

Beynon, K.I., D.G. Crosby, F. Korte, G.G. Still, J.W. Vonk, P.A. Greve. Environmental chemistry of pentachlorophenol. *Pure and Appl. Chem.* 53:1051-1080.

Blochel, A. 1992. Adsorption of halogenated phenolate ions to egg-phosphatidylcholine vesicles. Master's thesis, Portland State University.

Bruijn, J. and J. Hermens. 1990. Relationships between octanol/water partition coefficients and total molecular surface area and total molecular volume of hydrophobic organic materials. *Quant. Struct.-Act. Relat.* 9:11-21.

Callahan, M.A., M.W. Slimak, N.W. Gabel, I.P. May, C. Fowler, J.R. Freed, P. Jennings, R.L. Durfee, F.C. Whitmore, B. Maestri, W.R. Maybe, B.R. Holt, C. Gould. 1979. Water-Related Environmental Fate of 129 Priority Pollutants. U.S. Environmental Protection Agency: Washington, DC. Vol. I and II, EPA-440/4-79-029a and EPA-440/4-79-029b.

Chessells, M., D.W. Hawker, D.W. Connell. 1991. Critical evaluation of the measurement of the 1-octanol/water partition coefficient of hydrophobic compounds. *Chemosphere* 22:1175-1190.

Chiou, C.T., D.W. Schmedding, M. Mannes. 1982. Partitioning of organic compounds in octanol-water systems. *Environ. Sci. Technol.* 16:4-10.

Gerthsen, C, H.O. Kneser, H. Vogel. 1986. Physik: Ein Lehrbuch zum Gebrauch neben Vorlesungen. Springer Verlag, Berlin Heidelberg.

Geyer, H.J., I. Scheunert, F. Korte. 1987. Distribution and bioconcentration potential of the environmental chemical pentachlorophenol (PCP) in different tissues of humans. *Chemosphere* 16:887-899.

Hattemeyer-Frey, H., C.C. Travis. 1989. Pentachlorophenol: Environmental partitioning and human exposure. *Arch. Environ. Contam. Toxicol.* 18:482-489.

Herrmann F. 1993. Physik V, Thermodynamik. Universität Karlsruhe. Skripten zur Experimentalphysik.

Jafvert, C. and J.C. Westall. 1990. Distribution of hydrophobic ionogenic organic compounds between octanol and water: Organic acids. *Environ. Sci. Technol.* 24: 1795-1803.

Lagas, P. 1988. Sorption of chlorophenols in the soil. *Chemosphere* 17:205-216.

Leo, A., C. Hansch, D. Elkins. 1971. Partition coefficients and their uses. *Chem. Rev.* 71:525-616.

Mackay, D. 1982. Correlation of bioconcentration factors. *Environ. Sci. Technol.* 16:274-278.

Miller, M.M., S.P. Wasik. 1985. Relationships between octanol-water partition coefficient and aqueous solubility. *Environ. Sci. Technol.* 19:522-529.

Mussalo-Rauhamaa, H., H. Pyysalo, K. Antervo. 1989. The presence of chlorophenols and their conjugates in Finnish human adipose and liver tissue. *The Science of Total Environment* 83:161-172.

Nelson, A.P. and D.A. McQuarrie. 1975. The effect of discrete charges on the electrical properties of a membrane I. *J. theor. Biol.* 55:13-27.

Nicholson, D.K., S.L. Woods, J.D. Istok, D.C. Peek. 1992. Reductive dechlorination of chlorophenols by a pentachlorophenol-acclimated methanogenic consortium. *Applied and Environmental Microbiology* :2280-2286.

OECD, Organisation of Economic Co-operation and Development. 1981. Partition Coefficients. *In: Guidelines for testing of Chemicals*, 107, Paris, France.

Paasivirta, J., H. Tenhola, H. Palm, R. Lammi. 1992. Free and bound chlorophenols in kraft pulp bleaching effluents. *Chemosphere* 24:1253-1258.

Sabijic, A., H. Güsten, J. Hermens, A. Opperhulzen. 1993. Modeling octanol/water partition coefficients by molecular topology: Chlorinated Benzenes and Biphenyls. *Environ. Sci. Technol.* 27:1394-1402.

Schwarzenbach, R.P, W. Giger, C. Schaffner, O. Wanner. 1985. Groundwater contamination by volatile halogenated alkanes: Abiotic formation of volatile sulfur compounds under anaerobic conditions. *Environ. Sci. Technol.* 19:322-327.

Schellenberg, K., C.Leuenberg, R.P. Schwarzenbach. 1984. Sorption of Chlorinated Phenols by Natural Sediments and Aquifer Materials. *Environ. Sci. Technol.* 18:652-657.

Schmidt, P.O. 1995. Origins of effective charge of multivalent ions at a membrane/water interface and distribution of 2,3,4,5-Tetrachlorophenol in a membrane model system. Master's thesis, Portland State University.

Silverstein, R.M., G. C. Bassler, T.C. Morrill. 1991. Spectrophotometric identification of organic compounds. John Wiley & Sons.

Singer, S.J. and G.L. Nicolson. 1972. The fluid mosaic model of the structure of cell membranes. *Science* 175:720-731.

Sittig, M. 1985. Handbook of Toxic and Hazardous Chemicals and Carcinogens. *Noyes Publications*, Park Ridge, N.J.

Smejtek, P., K. Hsu and W.H. Perman. 1976. The electrical conductivity in lipid bilayer membranes induced by pentachlorophenol. *Biophys. J.* 16:319-336.

Smejtek, P. and S. Wang. 1993. Distribution of hydrophobic ionizable xenobiotic between water and lipid membranes: Pentachlorophenol and pentachlorophenate. *Arch. Environ. Contam. Toxicol.* 25:394-404.

Stryer, L. 1981. Biochemistry. W.H. Freeman and Company, San Francisco.

Terada, H. 1990. Uncouplers of oxidative phosphorylation. *Environmental Health Perspectives* 87:213-218.

Völker, D. 1994. Interaction of Ruthenium Red with Phospholipid vesicles. Master's thesis, Portland State University.

Wang, L., R. Govind, R.A. Dobbs. 1993. Sorption of toxic organic compounds on wastewater solids: Mechanism and modeling. *Environ. Sci. Technol.* 27:152-158.

Westall, J.C., C. Leuenberger, R.P. Schwarzenbach. 1985. Influence of pH and Ionic Strength on the Aqueous-Nonaqueous Distribution of Chlorinated Phenols. *Environ. Sci. Technol.* 19:193-198.

Westall, J.C., C.A. Johnson, W. Zhang. 1990. Distribution of LiCl, NaCl, KCl, HCl, MgCl₂, and CaC₂ between Octanol and Water. *Environ. Sci. Technol.* 24:1803-1810.

Wild, S.R., S.J. Harrad, K.C. Jones. 1992. Pentachlorophenol in the UK environment I : a budget and source inventory. *Chemosphere* 24:833-845.

Wild, S.R., K.C. Jones. 1992. Pentachlorophenol in the UK environment II: Human exposure and an assessment of pathways. *Chemosphere* 24:847-855.

Xie, T.M., B. Hulthe, S. Folestad. 1984. Determination of partition coefficients of chlorinated phenols, guaiacols and catechols by shake-flask GC and HPLC. *Chemosphere* 13:445-459.